Raman Spectroscopy as a Novel Technique for Non-Destructive Measurements of Transparent Materials in Bullet-Resistant Glass

Raman Spectroscopy as a Novel Technique for Non-Destructive Measurements of Transparent Materials in Bullet-Resistant Glass

Monika Wilson

A Thesis in the Field of Biotechnology

for the Degree of Master of Liberal Arts in Extension Studies

Harvard University

March 2020

Abstract

The hypothesis that Raman spectroscopy can be used to study bullet-resistant glass was proposed. Raman spectroscopy has been employed historically as a useful scientific inspection tool that reveals information about the molecular structure of a material. A long working distance Raman spectrometer was designed and built. The novel use of this device as a technique for the characterization of thick transparent materials is described. Experiments using the custom Raman system on bullet-resistant glass constructs and related samples are defined herein. The results are discussed in terms of the material identity, thickness and order within the multilayered constructs. The unique Raman signal is related to the identity of each material and demonstrated with the instrument. In addition, full depth profiles are created for complex samples of bullet-resistant glass. It is concluded that Raman spectroscopy is an ideally suited technique in these types of measurements that can be utilized beyond bullet-resistant glass samples. In conclusion, this method proved to be effective in supporting this thesis and may have much broader use with continued exploration.

Frontispiece

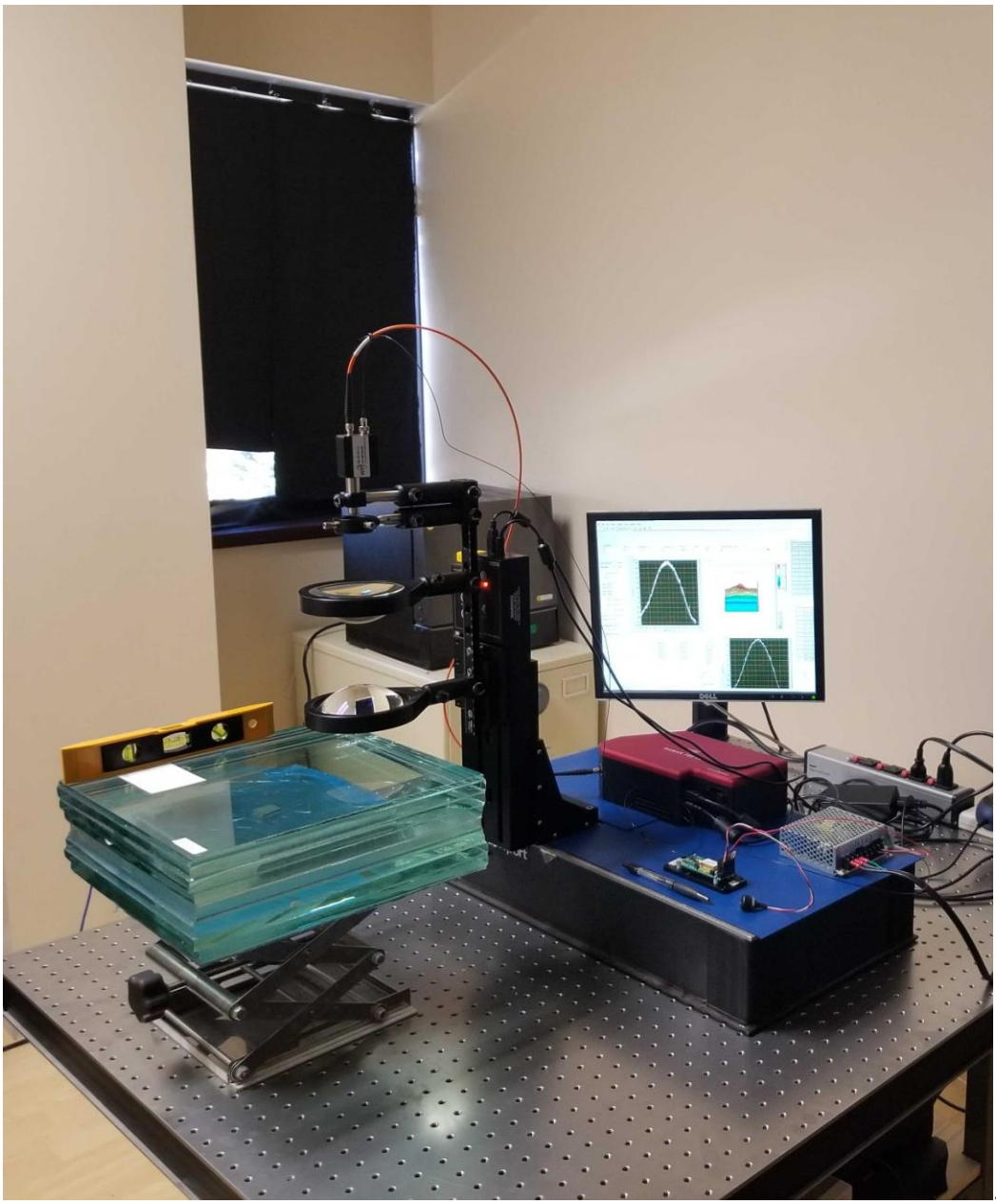 .

Author's Biographical Sketch

Monika Wilson has been working in the biotech industry for nearly a decade after matriculating from Tulane University in 2010 with a bachelor of science in biology. As she began her career in the sciences and the pursuit of innovation, it led her to the Harvard Extension School and this work.

Dedication

This thesis is dedicated in honor of my grandmothers.

My paternal grandmother, Dr. Jean Wilson, who studied at Cambridge University to study medicine in a time when women were only awarded titular degrees. She has been an immense inspiration in my life, in academics and in adversity.

And in honor of my maternal grandmother, Lucyna Ulecka, an immensely strong and savvy business woman who fought and escaped communism. Her strength in the midst of despair amazes and motivates me in life and in this work.

Acknowledgments

I would like to express my acknowledgement of all the people who supported this effort. I would like to thank my colleagues who inspired a spirit of research and intellectual excitement that allowed the conception of this work. Under the guidance of Dr. Wayne Weimer, his continual mentorship and passion for innovation, this thesis came together. In addition, I would like to acknowledge Dr. Steven Denkin, his expertise throughout this process and guidance in the early stages allowed this work to take flight. I am grateful to each person who helped contribute in practice or in patience with me and this project.

Table of Contents

List of Tables

List of Figures

Chapter I

Introduction

Although most people may not initially recognize the ubiquity of bullet-resistant glass, it is actually all around us. Bullet-resistant glass, commonly called bulletproof glass, is critical in the success and safety of all branches of the military, law enforcement and is useful to civilians. Bullet-resistant glass is classically thought of as armored protection for security; such ballistic-resistant glass can be found in tactical and armored vehicles, in bank windows, in museums to protect fine art and historically significant documents, in casino or gas station teller windows, high profile areas that may be targeted for attack or even in schools. However, in addition to protection from ballistics, it is also used across many other industries.

This type of glass may be used in areas or instruments where heat and pressure are of concern such as submarine or subterranean environments. In addition to protective properties, laminated glass is more effective at blocking ultraviolet radiation so it is used in aerospace and commercial aircraft applications or even domestic skylights. In severe weather prone areas it can be used to prevent damage such as hurricane-resistant construction. It is often used in building architecture, for example, high rises and exterior storefronts. Music venues will use laminated glass as sound insulation. It is also often found in high pressure ovens, vacuum chambers, and chemical hoods to name a few.

It is referred to as bullet-resistant glass, ballistic glass, bulletproof glass, transparent armor, laminated safety glass; as the user must be able to see through it but

also be protected from threatening elements. Although most people are largely unaware of these constructs around us, they play a significant role in our everyday life.

Bullet-Resistant Glass

Bullet-resistant glass is a common term for highly engineered structural composites that utilize multiple transparent materials to absorb the impact of a ballistic affront. A bullet-resistant glass construct can be made up of several layers of glass, plastics, transparent adhesives, polymer interlayers, antistatic discharge coatings, metallic mesh or transparent ceramics (Subhash, 2013). The design is often several inches thick and can weigh hundreds of pounds. While the glass layers provide a transparent material to view through, the majority of the energy from an impact is absorbed by the glass, the plastic and the polymer interlayers (Weller, 2005). The interlayers also contain the shattered glass in one piece to minimize shard induced damage. Each layer has been specifically designed using ideal materials for the application. In addition, each full stack up is also designed appropriately for the specific application (Freeguard, 1980).

A simple example of a layered laminated glass is an automotive windshield. The glass in automotive windshields is not the same as in a window pane of a home. It is designed with two transparent glass layers bonded with a single adhesive interlayer that allows it to flex when impacted but also holds together when the glass is shattered. This is called laminated safety glass to minimize the harm when it is impacted. These highly engineered materials are critical to the safety of passengers and are a similar design to the bullet-resistant glass we see in other applications. However, in vehicles designed for personal use, this laminated safety glass is not very thick and would be inadequate to slow down the impact of a bullet which would require more and thicker layers.

These laminated constructs can be found in applications where a firearm may be used to cause harm. They must be transparent and transmit an image undistorted to support their function as windows but also absorb the impact of a bullet if fired upon. In action, the bullet pierces the first layer of glass but a portion of the energy is absorbed by the glass and by the adhesive interlayer. Each subsequent layer absorbs an additional portion of the energy and the total construct is able to absorb all the energy before the bullet is able to exit the final layer, as seen in Figure 1. Different ratings of bullet-resistant glass are designed to withstand a specific amount of ballistic energy. With varying materials, thickness and number of layers the appropriate construct can be designed for the needs of the end user. The user must have complete confidence in the glass to be appropriate for the level of protection and also be confident in the quality since it is a protective material.

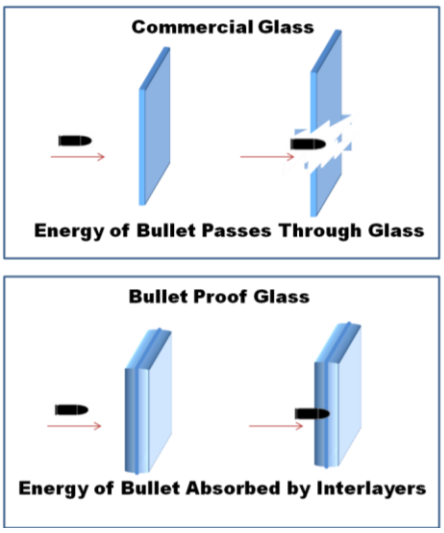

Figure 1. Bullet-Resistant Glass Schematic.

When a bullet hits a single pane of glass, energy from the speeding bullet is transferred to the glass causing it to break (top). In bullet-resistant glass, energy is absorbed by the glass and the adhesive interlayers (bottom).

The Problem

Once the bullet-resistant glass has been installed and deployed, it is not possible to non-destructively determine the structure of the construct, meaning the material composition, the thickness of each layer in the stack up and the stack up order. The ability to non-destructively characterize the bullet-resistant glass (for example, detect invisible delamination) is an important tool for both quality control and forensic analysis. In addition, it would be a useful analysis tool if the level of wear and tear or results of an impact could be characterized.

Due to the optical properties of glass and transparent materials, it may be a good candidate for optical probing. One such optical technique, Raman spectroscopy, may be an appropriate method to non-destructively and rapidly measure bullet-resistant glass in the field.

A useful technology will be capable of non-destructively measuring the types of materials that make up a transparent bullet-resistant glass sample, in the order the material appears in the stack up and be able to determine the thickness of each layer. A measurement such as this is relevant because it can characterize a piece of glass before it is installed in a vehicle to minimize the deployment of incorrect component parts. It will also be critical in characterizing materials that have already degraded and even failed after they have been in the field. A method and tool for characterizing bullet-resistant glass will allow for more rapid replacement but also can build a database of information about the conditions that lead to failure to aid in failure analyses. Should the method prove to be successful, it has applications outside of bullet-resistant glass

characterization. This method might be useful in other thick transparent materials in a way Raman spectroscopy has not been used before.

Raman Spectroscopy

The goal of this thesis was to design, build and test a Raman spectroscopy based platform that can characterize, identify and measure the thickness of, each layer of a bullet-resistant glass stack up. The hypothesis that Raman spectroscopy is an effective tool for measuring the thickness and make up of bullet-resistant glass was explored. In order to illuminate on this hypothesis, we explore the theory behind Raman spectroscopy.

Vibrational spectroscopy is a well known method of chemical analysis that can be used for many applications. Raman spectroscopy, a form of vibrational spectroscopy, is particularly well suited for characterization of transparent materials because of the scientific principles behind the method. Raman spectroscopy schematic seen in Figure 2.

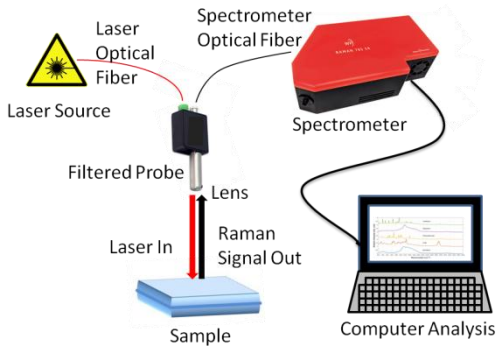

Figure 2. General Schematic of a Raman Spectroscopy Set Up

In this schematic, in 180 degree back scattering geometry, a laser illuminates a sample and a spectrometer detects the Raman signal from the sample which can then be interpreted through computer analysis.

Raman spectroscopy is based on inelastic scattering of laser light. When light is scattered from a molecule, most photons are elastically scattered without any change in their energy or wavelength. This is known as Rayleigh scattering. However, a small fraction of light can be inelastically scattered by the molecules due to the vibrational energy of the chemical bonds that make up the molecule. Incident photons of the excitation laser light are annihilated by the sample and then scattered photons are emitted via the scattering process. The frequency of the emitted photons is shifted up or down in comparison with the original monochromatic frequency, which is called the Raman Effect. The difference in frequency between the incident photon and the Raman scattered photon is equal to the frequency of vibration of chemical bonds in the scattering molecule. The Raman shift therefore provides information about vibrational, rotational, and other low-frequency transitions in molecules. Since the measured Raman spectrum is a direct result of the bonds present in a molecule, it is a direct, unique and unambiguous identification of the molecules being probed, often called a fingerprint. The fingerprint region of a spectrum, between 400 cm^{-1} and 1800 cm^{-1}, can be used to differentiate between materials that may look identical to the human eye but are drastically different when comparing Raman spectrum. A sample can thereby be compared to a library of known materials to unambiguously determine the material identity.

Transparent materials are particularly suited for this methodology. The materials are all optical materials by the nature of their purpose; in order to see through them without distortion, they all have a refractive index of close to 1.5 and easily allow light to enter and return to the detector. However, because of the nature of Raman and the fingerprint region, the spectrum will demonstrate unique and unambiguous identification

for each material, even in the case of complex multilayered materials such as bullet-resistant glass. One aspect that often limits the use of Raman is that it relies on getting light in to a sample and then retrieving signal back. Some opaque or black materials fully absorb the light and diminish the returned Raman signal. However, in this optimal case of transparent materials, much of the signal can be retrieved thus enabling characterization of thick pieces of bullet-resistant glass.

Characterization of Transparent Materials in the Literature

From the literature, there is evidence that Raman is likely to be a successful tool for identifying transparent materials as it has been successful with similar materials in different applications historically (Strassburger, 2010). Raman spectroscopy has been demonstrated for measuring the identity and thickness of thin films in several studies (McCarty, 1987). It has been used to identify the materials found in transparent artifacts. It has been used to measure ice thickness. However, in the literature, Raman spectroscopy of this type has not been used to measure thick layers (up to 4 inches) of multiple and complex materials in a stack up. The following sections will discuss several historical studies that are the foundation for this work.

Identification of transparent materials with Raman Spectroscopy

In 2014, a study used Raman spectroscopy and XRT as methods for identifying polymers and plasticizers in goggles, flight helmets, airplane windows, and canopies in Smithsonian historic collections (Madden, 2014). The study probed historic materials used to create transparent plastic objects in the early-20th century. Because these items are highly valued specimens at the Smithsonian, the study heavily relied on the non-

destructive Raman spectroscopy tool for non-invasive analysis of these artifacts. The study demonstrates that Raman spectroscopy is a valuable tool for objectively and non-destructively measuring historic plastic compositions, including unknown formulations. The Raman data was combined with archival research of historical documents to identify window materials including glass, laminated safety glass, and sheets of plasticized cellulose nitrate, plasticized cellulose acetate, and polymethyl methacrylate (PMMA). As a result of this work, the Smithsonian routinely uses Raman spectroscopy to identify plastics. The construct of modern bullet-resistant glass is not the same as the historic pieces of the past, however, it is relevant that Raman was a successful tool for studying plastics and plasticizers of windows, goggles and cockpits. Building on this evidence, the proposed technology will be able to measure modern transparent materials used in thick bullet-resistant glass including when the materials are layered, while also measuring the thickness of each material in a stack up.

Metrology of Thin Films with Raman Spectroscopy

Although the concept of measuring thin films with Raman spectroscopy is not very different from the idea of measuring thick films in terms of application, the method is very different. Because of the focal point and the working distance and the entire range of the material, conventional measurements that are possible on thin films are not possible with thick stack ups. However, thin film research is an important part of material science, and semiconductor research and there has been significant research in to using Raman spectroscopy to measure thin films.

A thin film study using Raman spectroscopy was successfully able to measure thickness as related to Raman spectrum intensity. (Bugaev, 2012). In this case, the group

was studying the chemical species of Silicon deposited on to a wafer and then measured by Raman spectroscopy. They were able to correlate the intensity of the different Raman peaks to the species of Si present and the thickness they had deposited by the intensity of the Raman signal. Although this method will not apply to thick samples, there is evidence that the intensity will give information on the boarders of the materials and the depth profile of the bullet-resistant glass. This concept can be translated to the proposed technology where the layer thicknesses and sequences will be determined by the Raman signal.

Measurement of Ice with Raman LIDAR

In a study of arctic ice melting, a group was successful in verifying the thickness of ice using Raman scattering. In the study, the researchers use a layer of ice between air and water as one stack up and Polymethyl Methacrylate between air and water as a second sample (Pershin, 2015). The set up uses Raman LIDAR and performs the measurements at a distance. Raman LIDAR is a technique for surveying at a distance. It employs a pulsed laser and detects the scattered light using a 180 degree back scatter optical geometry, the same as in conventional Raman. However, similar to RADAR, it uses the differences in pulsed laser time and returned signal time to characterize the target. The difference between the Raman spectra of poly methyl methacrylate (PMMA) and water, and between ice and liquid water were employed to locate the PMMA-water and ice-water interfaces. Elastic scattering was used to detect the interface between air and the surface of PMMA or Ice. Their approach yields promising data for a remote and noninvasive thickness measurement technique in the field. Impressively, this is the only study in the literature that used Raman of any sort to measure the thickness of thick

materials. The Raman LIDAR method is perhaps more useful in situations such as emergency responders approaching rescues on ice, since the measurements can be made from multiple meters away, such as from a helicopter. It would be possible to lower a ruggedized version of the proposed Raman instrument on to ice and measure the thickness and thereby determine safety. Other situations that require an accurate identification and thickness measurement of transparent materials can also be envisioned.

Similar Applications

The proposed technology is useful for characterizing bullet-resistant glass but it is not limited to that application. The tool may also be used as a Quality Control (QC) device in deployment of transparent materials, such as architectural materials, or safety equipment such as lab safety hoods, lab glass, sporting equipment, tempered glass cookware, or glass furniture.

In addition to characterizing the thickness and layer sequences of materials, the anticipated technology will be able to locate contamination within layers and deterioration and delamination of materials over time. The Raman measurement relies on inelastic scattering for characterization but there is also elastic scattering at the measurement site. Any defects, air bubbles or contamination within the layers can be located quickly by measuring the elastic scattering or simply reflectance. Any changes in the reflectance will indicate contamination and the nature of the contamination can be determined using the Raman signal.

This would be very helpful as a method of quality control when installing tempered architectural or building glass. Spontaneous breakage of architectural glass used in construction can be attributed to multiple sources, one of which is inclusions.

There are more than 50 types of inclusions in float glass that can lead to spontaneous breakage. A particular inclusion called nickel sulfide stone, example in Figure 3, can cause spontaneous breakage and there is no known technology that can completely eliminate its formation in float glass in production (Vitro, 2014). Therefore, a method of QC that can detect this defect before installed would greatly improve the quality of the building and eliminate dangerous situations and costly repairs. As technology advances new and more applications can be imagined. It is anticipated that with the success of this work, more possibilities can be explored.

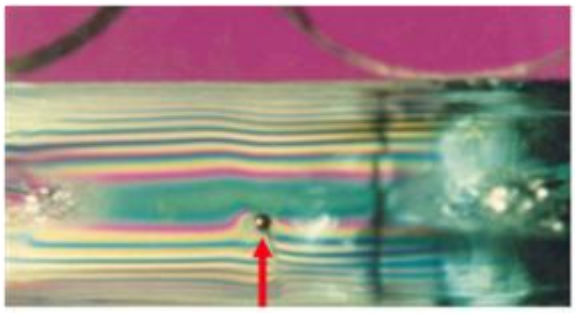

Figure 3. Nickel Sulfide Stone

Nickel Sulfide Inclusion seen in architectural glass (0.003" inclusion (Vitro Coatings Glass Technical Document)

Chapter II

Research Methods and Materials

In this section, the materials and methods used in the study will be detailed. Advanced optical spectroscopy techniques, material analysis and computational modeling were used in completion of this study. This work was conducted with the appropriate laser safety protocols observed in a modern optics laboratory. In short, a long working distance Raman system was designed and developed and several bullet-resistant glass samples were examined and analyzed on the system.

Objective

The overall objective of this study is to demonstrate that Raman spectroscopy can be used as a novel technique for non-destructively measuring thick layered transparent samples, such as those used for bullet-resistant glass. In order to provide evidence and prove this thesis, assessing the ability of Raman spectroscopy to produce data that enables full characterization of multilayered bullet-resistant glass, several methods and materials were necessary.

Raman System and Technique

The Raman spectrometer used in this technique was a Wasatch Photonics 785 Extended Range Spectrometer (WP 785 ER Raman Spectrometer). The instrument has a measurement range from 20 cm^{-1} to 3600 cm^{-1}. This particular model was selected in

order to capture the signal beyond what is called the Raman fingerprint region typically described as between 400 cm^{-1} and 1800 cm^{-1}. Capturing the signal from 1800 cm^{-1} to 3600 cm^{-1} allows for the possibility of additional Raman signal that may be helpful in distinguishing materials of similar but different molecular structure. The laser used was a 785 nm wavelength stabilized laser (Ondax OEM-785-PLR600-FCPC-2 Narrow Linewidth Multimode). The Raman probe was a Wasatch Photonics f/1.3 matched Raman probe with integrated filter set for 785 nm Raman measurements, but the probe external optics were custom designed for this Raman technique.

The Raman technique applied in this study was a novel method in which a long working distance was created through a series of lenses. The ultimate goal is to measure through a 4-inch-thick piece of bullet-resistant glass with high spatial resolution at the focal plane of the optical system perpendicular to the optical axis. In order to do this, the working distance must be greatly expanded compared to commercially available Raman probes. In many Raman systems, a small probe focuses a collimated laser beam onto the sample. This can be done a multitude of ways but commonly a lens or microscope objective is used. The lens focal length thereby determines the working distance. In this case, the working distance needs to be 4 inches or greater, as we anticipate samples of that thickness. In order to achieve this, the beam must be expanded and refocused.

For this experimentation the commercially available probe from Wasatch Photonics was used with this system. The lens contained in the probe assembly will be called L1. In order to optimize the resolution and minimize the signal loss, Lens 2 (L2) and Lens 3 (L3) were selected to match L1 in terms of optical power or f-number. The hardware in this optical set up was experimentally optimized.

As can be seen in Figure 4, the optical train utilizes two 100 mm diameter 100 mm focal length aspheric plano convex lenses (L2 and L3) that form a beam expander and collimator to produce a laser beam focus that is able to traverse samples up to four inches thick. The optical loss through the lenses is minimal, about 15 mW or 5%. The laser power was measured before the pinhole to be 300 mW and at the sample 285 mW. The pinhole is a 200 μm pinhole located between the first and second lens at the laser beam waist. The Raman probe and the two large aspherical anti-reflection coated plano-convex lenses form the system along the optical axis and are fixed in space on an optical rail mounted on a vertical computer-controlled translation stage.

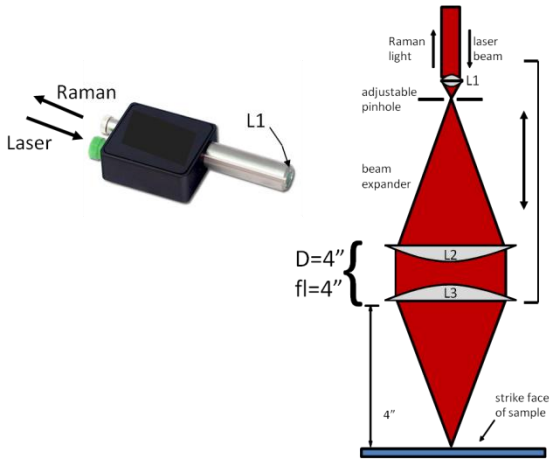

Figure 4. Raman Probe Design.

Filtered Raman Probe Schematic (left) Schematic of the Long Working Distance (right). Note three lenses used as a beam expander in the system. This novel Raman probe is necessary to penetrate and focus through 4 inches of sample.

The translation stage is capable of 150 mm travel needed for thick samples. The vertical translation stage is driven by a built-in stepper motor and can be programmed to increment any distance down to 5 microns between Raman measurements to obtain sufficient spatial resolution when constructing Raman depth profiles. The translation stage control program was written in LabView2018 and the stage was purchased from Thorlabs (Model LTS150). The precision of the stage is critical in the measurement as the stage travel will be correlated to the sample thickness.

Test Samples

The initial materials were comprised of single sheets of materials commonly found in bullet-resistant glass. These included varying thicknesses of borosilicate glass (Borofloat®), low iron soda lime glass (Starphire®), polycarbonate (ePlastics®), polyvinyl butyral (Butvar® B-98) as well as urethane (Krystalflex® PE399). One solid 32.66 mm piece of 4”x4”bullet-resistant acrylic from ACME Plastics was also acquired. In addition to these, two layered stack ups of 12"x12" commercially available bullet-resistant glasses were obtained from Standard Bent Glass: GCP Bullet-resistant UL Level 4 and GCP Bullet-resistant UL Level 8. Four other stack ups were fabricated by Standard Bent Glass to be representative of real-world bullet-resistant glass. An examples of these materials can be seen in Figure 5. The recipes are comprised of the same materials in different stack up orders with 10 layers and 9 interlayers totaling to 19 layers each. The samples and recipes are listed in Table 1 and Table 2.

Figure 5. Bullet-Resistant Materials

Bullet-Resistant Glass Recipe #3 (left) 32.66 mm Bullet-Resistant Acrylic (right)

Table 1. Recipes of UL 4 and UL 8 Bullet-Resistant Glass

Layer	**UL 8: 2"**	**UL4: 1 3/16"**
1	1/8" Heat Strengthened Glass	1/4" Annealed
2	.030 PVB	.030 PVB
3	3/8" Annealed Glass	3/8" Annealed
4	.030 PVB	.030 PVB
5	3/8" Annealed Glass	3/8" Annealed
6	.030 PVB	.050 Urethane
7	1/4" Annealed Glass	1/8" Polycarbonate AR1
8	.050 Urethane	
9	1/8" Polycarbonate	
10	.050 Urethane	
11	1/4" Annealed Glass	
12	.050 Urethane	
13	1/4" Polycarbonate AR1	
14	.025 Urethane	
15	1/8" Polycarbonate AR1	

The table lists the materials in the commercially available UL4 and UL8 materials as provided by the manufacturer

Table 2. Bullet-Resistant Recipe #1-4

Layer	Bullet-Resistant Recipe #1	Bullet-Resistant Recipe #2	Bullet-Resistant Recipe #3	Bullet-Resistant Recipe #4
1	6 mm Clear glass	6 mm Clear glass	6 mm Low Iron	6 mm Low Iron
2	30 mil pvb	25 mil S-123	30 mil pvb	25 mil S-123
3	12 mm Low Iron	11 mm Borofloat	12 mm Clear glass	12 mm Low Iron
4	25 mil S-123	30 mil pvb	25 mil S-123	30 mil pvb
5	12 mm Low Iron	12 mm Low Iron	12 mm Low Iron	12 mm Low Iron
6	25 mil PE399	25 mil PE399	25 mil PE399	25 mil PE399
7	12 mm Clear glass	12 mm Clear glass	Clear glass	11 mm Borofloat
8	50 mil PE499	50 mil PE499	25 mil S-123	50 mil PE499
9	3/8" Acrylic	1/8" polycarb	12 mm Low Iron	3/8" Acrylic
10	25 mil PE399	25 mil PE399	25 mil PE399	25 mil PE399
11	1/8" polycarb	3/8" Acrylic	1/8" polycarb	12 mm Clear glass
12	50 mil PE399	50 mil PE399	50 mil PE399	50 mil PE399
13	11 mm Borofloat	12 mm Low Iron	11 mm Borofloat	12 mm Clear glass
14	25 mil S-123	25 mil PE399	50 mil PE499	25 mil S-123
15	12 mm Low Iron	12 mm Low Iron	3/8" Acrylic	12 mm Low Iron
16	25 mil PE399	25 mil S-123	25 mil PE399	25 mil PE399
17	12 mm Clear glass	12 mm Clear glass	12 mm Low Iron	1/8" polycarb
18	50 mil PE-399	50 mil PE-399	50 mil PE-399	50 mil PE-399
19	1/8" AR1 Poly	1/8" AR1 Poly	1/8" AR1 Poly	1/8" AR1 Poly

Table 2 displays the recipes of 4 bullet-resistant glass constructs designed for this experiment.

Computational Analysis

The novel concept of this thesis lies in the long working distance of the Raman platform. In order to determine the likelihood of success in this study, computational modeling was explored using COMSOL Multiphysics modeling software. COMSOL is a simulation and solver software used in simulating physics based models. In this instance, the COMSOL Ray Optics Module was utilized to simulate the laser light and return Raman signal through a series of lenses designed to expand the laser light and create a long working distance in order to allow travel through a thick piece of bullet-resistant glass. A conventional Raman probe would only be able to probe the surface and near

surface areas of the sample, however through the modeling it was shown that the expanded beam will traverse fully through a thick sample. In addition, various lens types and orientations of the optics could be simulated to optimize the system before physical experimentation. The measurements and properties of the lenses and materials can be imported in to COMSOL from the manufacturers' engineering drawings. This allows the model to provide excellent accuracy and predictive power which is very useful when building an optical system.

In addition to the modeling, computational analysis was also used on the experimental data. Microsoft Excel, Origin Pro, MATLAB and COMSOL Multiphysics were used in the data analysis for this report and for generating plots used herein.

Measurement Protocol

In order to ensure accurate results, the measurement protocol was standardized. There was no sample preparation necessary as the method is a direct measurement of the bullet-resistant glass. The sample was placed on a stage at the base of the instrument. In the case of multi-layered constructs, the polycarbonate plate was oriented on the bottom. The polycarbonate plate can be identified by eye as the cut edge is not smooth like the glass layers. The sample was then brought into focus of the laser beam by use of a reticle, the location will vary with thickness of the sample. Using LabView2018, the step size of the motorized stage and the integration time was set. The step size of the motorized stage can be varied depending on the sample. However, in the case of the thicker samples and those known as Bullet-resistant Recipe #1-#4, the step size was set to 0.10 mm. The number of pre-programmed measurement loops was determined roughly by the total thickness of the sample divided by 0.10 mm. The integration time for each Raman

measurement was set to 100 ms. The laser power was set to 300 mW for all measurements. Ambient light was minimized with black out curtains and room lights off during measurements. Appropriate eye protection for laser safety was utilized and the lab was secured for the safety of others. Automated measurements were initialized using the protocol in LabView2018 and measurement progress was monitored. All measurements were recorded and saved for further analysis.

This protocol was developed over the course of experimentation in order to optimize the measurements. Further details on the experimental design will be detailed in the next chapter of this thesis titled Results. In addition to collecting the data, further analysis was performed with the data collected that will also be described in subsequent sections of this report.

Chapter III

Results

The long working distance Raman system was designed and assembled using Commercial Off the Shelf (COTS) items described in the previous section. The software was developed with large data set collection in mind. The system in total was verified and validated against real-world bullet-resistant glass and representative materials.

Hardware Design and Assembly

The spectrometer and laser were preselected through a trade study of the requirements and commercially available options. The chosen spectrometer was Wasatch Photonics 785 Extended Range Spectrometer (WP 785 ER Raman Spectrometer). The final selection of the laser was an Ondax butterfly laser (OEM-785-PLR600-FCPC-2 Narrow Linewidth Multimode).

The laser itself was experimentally determined to need at least 300 mw at 785 nm excitation wavelength to provide adequate signal in 100 ms of integration. The laser fiber was a 1 meter long fiber NA 0.22 and 105 μm diameter. The size of the pinhole was determined by experimentally generating a beam profile of the laser. The laser waist size was determined to be approximately 200 μm so a 200 μm pinhole was used (Thorlabs). The goal of the pinhole was to allow as much of the laser beam as possible to reach the sample but only the focused portion of the Raman signal to return, this allows for better spatial resolution which was critical in the success of the instrument.

The fiber optic used for the spectrometer was a 1 meter long fiber NA 0.39 and 600 μm diameter to match the spectrometer requirements. The Raman probe was commercially available and matched to the spectrometer from the same company, Wasatch Photonics, described previously in this report as a Wasatch Photonics f/1.3 matched Raman probe with integrated filter.

The assembly required alignment of the optical train from the laser, through the pinhole, through the optics and back through to the Raman spectrometer. With a series of progressive steps yielding the greatest Raman signal, the system was optimized. The optimal laser power and integration time was also established by determining the best tradeoff between signal to noise and resolution of the spectra by measuring known materials such as silicon and acetaminophen as standards, as is common practice in Raman spectroscopy methods. In addition, the step size needed for spatially resolving in the focal axis was experimentally determined with the test samples. The final experimental parameters were established as 300 mw laser power, 100 ms integration time and 0.1 mm step size. The set up can be seen in Figure 6 and Figure 7.

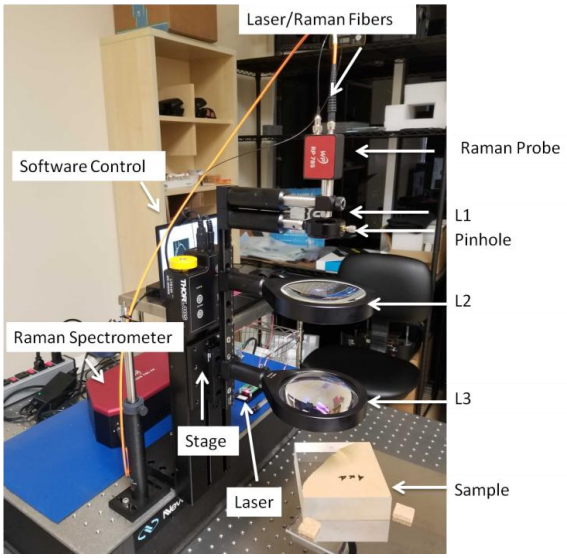

Figure 6. Labeled Set Up

Note the probe at the top of the optical train, L1, pinhole, L2, L3, and the focus on the sample at the bottom of the optical train. The translation stage, laser, Raman spectrometer and software control can all be seen in this image.

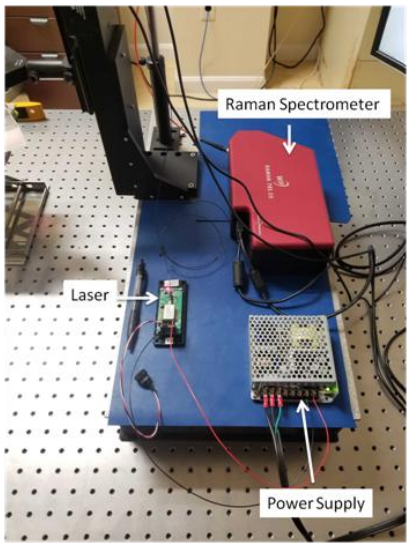

Figure 7. The Raman Spectrometer, Laser and Power Supply

Wasatch Photonics spectrometer (785 ER), laser (Ondax) and power supply

Software Development

System control software was developed in LabView2018 to control the stage movement and the integration time. By creating custom software, the step size could be easily changed until the optimal distance was established. The stage, Thorlabs Model LTS150, provides a .NET control framework that can be integrated into LabView and further customized. In addition, the automated measurements were extremely accurate and repeatable which was essential because of the volume of data collected for analysis.

Once the initial set up of the long working distance Raman system was complete and the control software was implemented further experimentation in support of this thesis began. The entire system is seen in Figure 8.

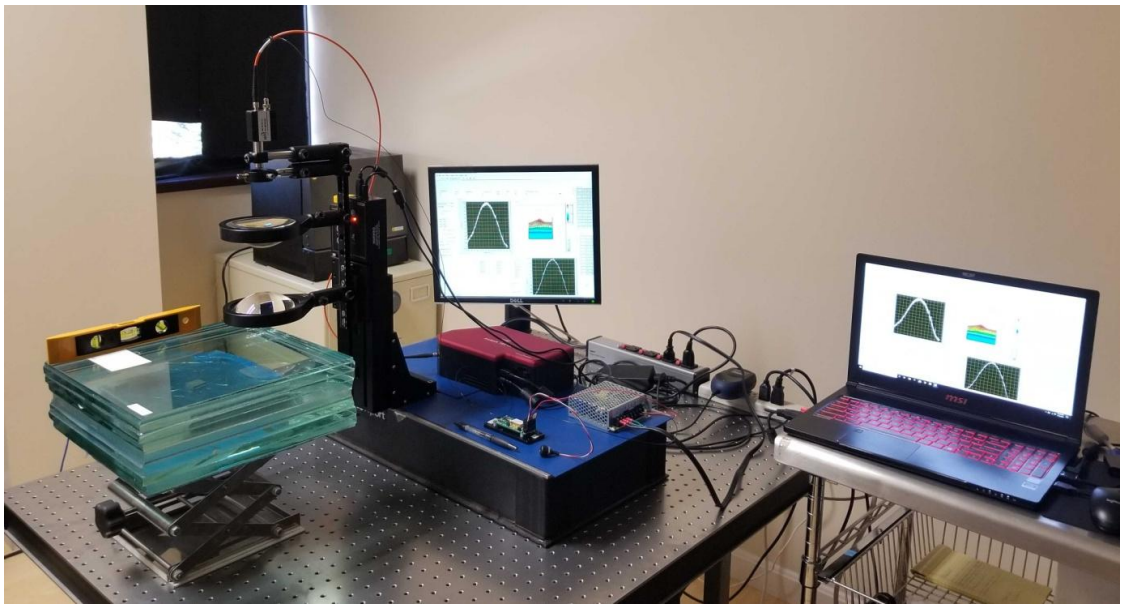

Figure 8. The Long Working Distance Raman Depth Profiling Platform.

In this imagine, the fully functional system of the long working distance Raman depth profiling platform is shown.

Experimental Goals

The first aim was to assess feasibility. By collecting preliminary data and running computational models, the likelihood of success could be determined. After feasibility had been demonstrated, the experimental aim was to test the platform using real world layered samples of bullet-resistant glass. The final task was to analyze the data and evaluate the thesis that Raman can be used as a novel technique for characterizing thick specimens of bullet-resistant materials.

Feasibility Study

In order to obtain preliminary data to determine feasibility of the thesis, an exploratory experiment was conducted on several commercially available transparent materials that are common in bullet-resistant glass. There was evidence in the literature cited previously that Raman is a good tool for investigation of transparent materials and thickness measurements. Transparent materials such as PMMA and ice were shown to have been measured successfully with forms of Raman spectroscopy providing some evidence for feasibility.

If the hypothesis is true, then simple samples of transparent materials will have a feature-rich Raman signal and the broader thesis that it can be used to measure more complicated bullet-resistant glass constructs is feasible. The scope of this initial experiment was to acquire Raman spectra of commercially available materials including: borosilicate glass (Borofloat®), low iron soda lime glass (Starphire®), polycarbonate (ePlastics®), urethane (Sigma-Aldrich), and polyvinyl Butyral (Butvar® B-98) as well as urethane (Krystalflex® PE399). The collected spectra were validated against historic Raman spectra from the literature where possible.

In figure 9 below, the Raman spectra of five of the aforementioned materials are displayed. The Raman signal was collected with a conventional Raman spectrometer and is a surface measurement of the bulk Raman signal. The x-axis shows the Raman shift in cm^{-1} from the laser line. The y-axis is in arbitrary units showing the intensity of Raman signal at each wavenumber. The spectra have been offset for visual clarity. As discussed earlier, the molecular structure of the materials directly give rise to the Raman spectrum. A suitable Raman signal is one where there are identifiable Raman peaks with enough intensity to identify and distinguish them from other materials.

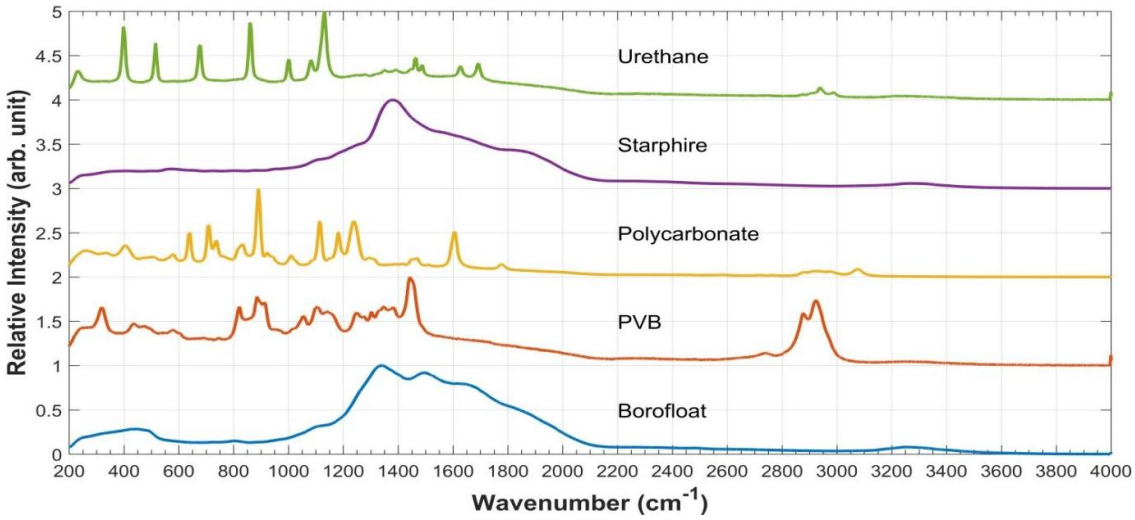

Figure 9. Bulk Raman Spectra of Bullet-resistant Glass Materials

Raman Spectra of 5 materials taken with a conventional Raman Spectrometer

Based on the spectra collected it was determined that there were plenty of available features in the spectrum to distinguish the different materials from each other. By visual analysis between each spectrum, the Starphire and Borofloat (glass samples),

have broad features that differ greatly from the adhesive materials and polycarbonate that are feature rich in the Raman fingerprint region, between 400 cm^{-1} and 1800 cm^{-1}. In addition, each spectrum has unique peaks that can be used to distinguish materials from each other. This preliminary evidence justifies further exploration and testing of the hypothesis that Raman spectroscopy will be a successful tool in measuring thick assemblies of bullet-resistant glass.

In order to explore the functionality of the long working distance, thicker samples of the above materials were examined using the long working distance Raman platform. The following figures will demonstrate those materials. In each depth profile, a single layer of transparent material is measured. Each one demonstrates unique Raman signature. Low iron (LI), also known as low iron soda lime glass, has a distinctive peak and shoulder at 1382 cm^{-1} and 1846 cm^{-1} respectively. The borosilicate glass peaks are in the same area but seen by a doublet of peaks at 1342 cm^{-1} and 1494 cm^{-1}. The adhesive interlayer peaks that are most easily seen are at 2864 cm^{-1} and 2920 cm^{-1} for PE399 and 2877 cm^{-1} and 2920 cm^{-1} for PVB as well as features in the fingerprint region. Multiple polycarbonate peaks are visible between 200 cm^{-1} and 1400 cm^{-1}. Acrylic has features in the fingerprint region that is unique and different than the polycarbonate. There are many other peaks that can be tracked mathematically, ensuring material identification and thickness, but these will be sufficient for visual clarity.

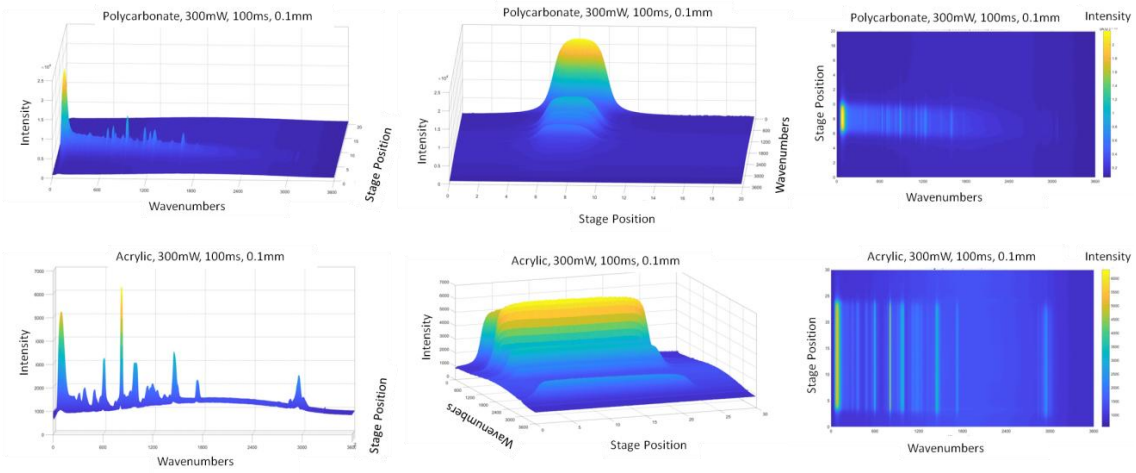

Figure 10. Raman Depth Profile of Plastics

6 mm polycarbonate (top) front image of Raman spectra (top left), Side view of depth profile demonstrating thickness (top middle) top down view demonstrating thickness (top right) 32.66 mm Acrylic (bottom) front image of Raman spectra (bottom left), Side view of depth profile demonstrating thickness (bottom middle) top down view demonstrating thickness (bottom right)

The materials above, in Figure 10, are two plastic components commonly found in bullet-resistant glass. The acrylic itself can be used as a bullet-resistant material in some situations. These two samples are feature rich in the Raman fingerprint region. Each material has different peak patterns that can be used to distinguish from one another. In addition to that it is of note that the Polycarbonate sample is 6 mm thick and shows a drastic contrast to the 32.66 mm Acrylic sample in the top down view. These two samples provide sufficient evidence that the long working distance Raman platform will be useful for measuring both relatively thick and thin plastic materials in bullet-resistant glass.

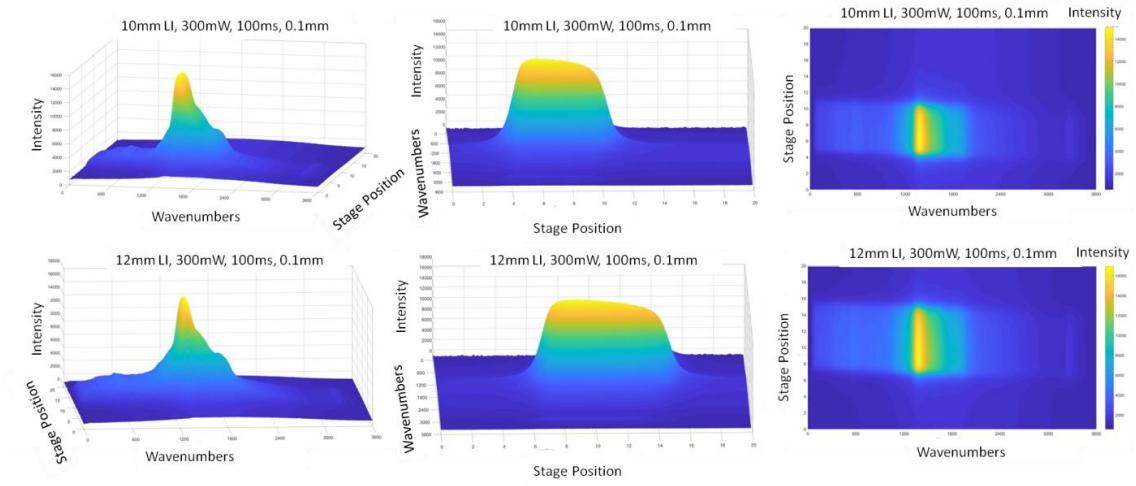

Figure 11. Raman Depth Profile of Low Iron Soda Lime Glass

Raman depth profiles of two thicknesses of low iron soda lime glass are pictured here. 10 mm LI Raman Spectra demonstrating a large peak and shoulder at 1382 cm^{-1} and 1846 cm^{-1} respectively (top left). 10 mm LI depth profile from the side demonstrating 10 mm thickness (top middle). A top down look at the depth profile demonstrating thickness (top right). 12 mm LI Raman Spectra (bottom left). 12 mm LI depth profile from the side demonstrating 12 mm thickness (bottom middle). A top down look at the depth profile demonstrating thickness (bottom right).

The thickness of the material can be correlated to the stage position. With each collected spectrum, the focus moves further into the sample, so when the signal change approaches zero, it indicates the measurement focus has fully traversed and is no longer in the sample. In Figure 11, with two different thicknesses of LI glass, it is clear that this system is able to measure thickness as the 12 mm LI glass has a thicker depth profile than the 10 mm LI glass depth profile as can be seen by the Raman depth profiles above.

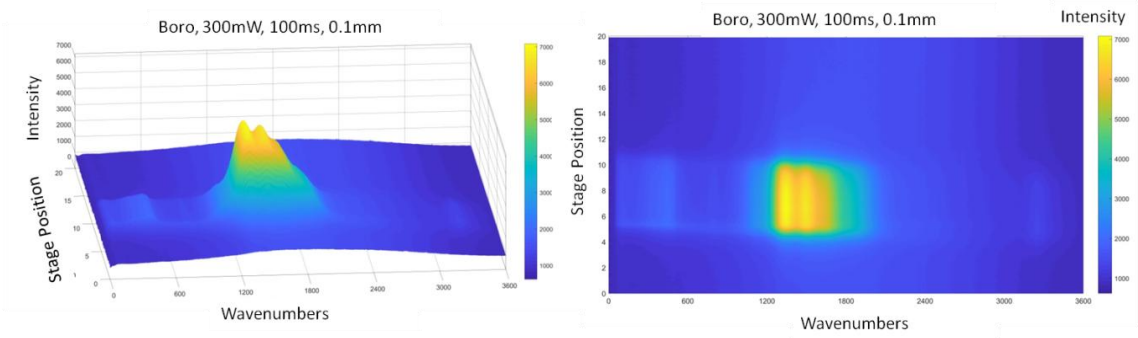

Figure 12. Raman Depth Profile of Borosilicate Glass

Note the doublet peak feature in borosilicate glass that it significantly different from low iron soda lime glass. This study shows us that different glass types are distinguishable with this system.

Each of the adhesive layers have a peak in the spectrum around 2800 cm^{-1} - 2900 cm^{-1} depending on the type of adhesive. This peak is useful because the other materials do not have significant peaks in that area of the spectrum. These peaks can be seen most clearly around 0.5 mm as they start, rise and then end. In addition, the adhesive layers have many other features in the fingerprint region that can be tracked. The adhesive layers can also be identified because they are much weaker in signal to the glass layers. This is in part because they are relatively thin and Raman is a quantitative measurement. However, there is plenty of feature apparent that can be tracked in the full depth profiles, as can be seen in Figure 13.

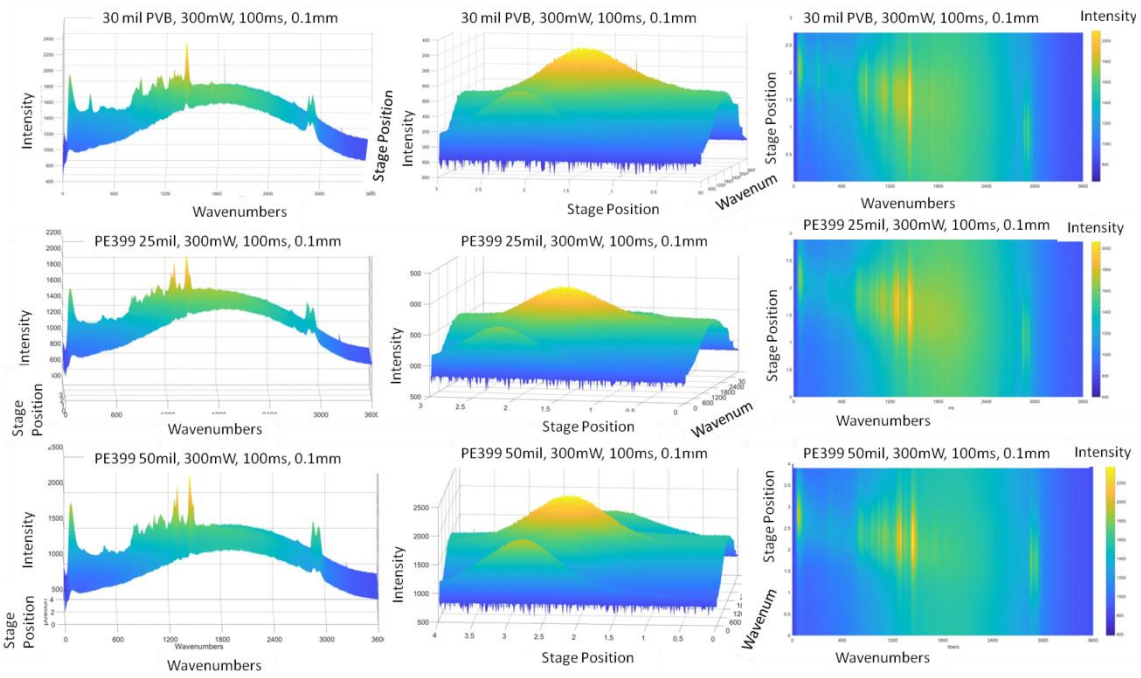

Figure 13. Adhesive Layer Raman Depth Profiles

30 mil PVB (top), 25 mil urethane (PE399) (middle), 50 mil urethane (PE399) (bottom). There spectrum of the PVB adhesive is notably different than that of urethane (PE399). Note the corresponding spectra in the urethane samples.

With the data collected in this first experiment, there is sufficient evidence to believe this system will be successful with complex samples. The long working distance Raman system clearly characterized single sheets of materials commonly found in bullet-resistant glass and further measured through thick samples of these single materials.

COMSOL Multiphysics Modeling

As described previously, COMSOL Ray Optics Module was used to model the system and the ability of the lenses to successfully traverse a thick sample vs. conventional Raman which is only able to probe the surface of a sample. The series of

lenses are specified in the model as well as the laser source and pinhole. The laser can be simulated in multiple ways, in the example below it is demonstrated as a ribbon from the source.

As can be seen in the figure below, a four-inch piece of soda lime glass is specified in the model. The figure on the left shows where the focus would be if there were no glass block and the laser is simply focusing in air. The laser beam in the model is then moved partially into the glass block. As the beam moves into the block, the working distance lengthens, and the focus is shifted lower. When the beam completely passes through a 4 inch glass block, the focus is shifted past the block and focuses outside of the glass block. This is an advantage in this case as it allows the focus to reach through the entire sample. However, this means that the stage distance is not directly equivalent to the thickness measurement, an shown in Figure 14.

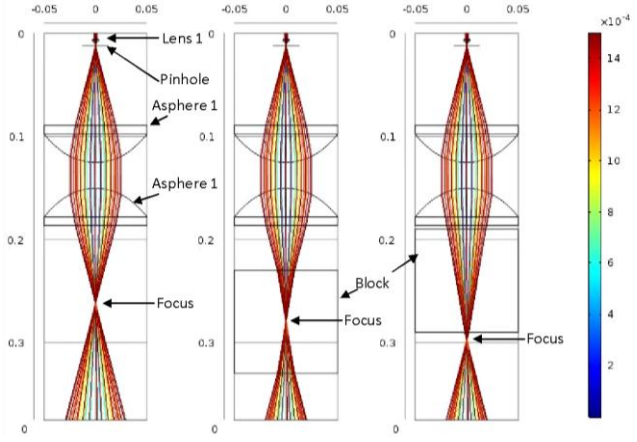

Figure 14. Ray Trace Diagrams

Ray trace diagrams with no glass block (left). Partially in glass block (middle). Fully in glass block (right).

Bullet-resistant Glass Sample Experimentation

The modeling suggests that we will be successful in measuring through an entire section of bullet-resistant glass that is four inches thick. With this data and the initial Raman signal collected from the materials, it is reasonable to believe that the long working distance Raman system will be able to successfully measure through multilayer bullet -resistant glass samples.

The following Raman depth profiles of the previously described samples demonstrate that Raman is in fact a suitable tool for characterizing bullet proof glass. The plots show the as collected Raman spectra, displayed with the first spectrum taken by the probe in the back, where the signal is notably higher, to the front which is the last plate in the stack up and deepest in the sample. In the following images you will note that some materials have a larger Raman cross section. The intensity of the signal is dependent on the material itself, as well as its position in the stack up.

UL4 is a commercially available and commonly used bullet-resistant glass. It is comprised of 3 layers of annealed soda lime glass, with the second layer being the thicker than the first and equal in thickness to the third with one single layer of polycarbonate held together by 3 adhesive layers. In Figure 15 below, these features are easily distinguishable by eye, the thick layers of soda lime annealed glass clearly distinguishable by the large broad peak around 1382 cm^{-1} with valleys in between representing the thin but present adhesive layers and finally the feature rich peaks of the polycarbonate visible in the front of the depth profile.

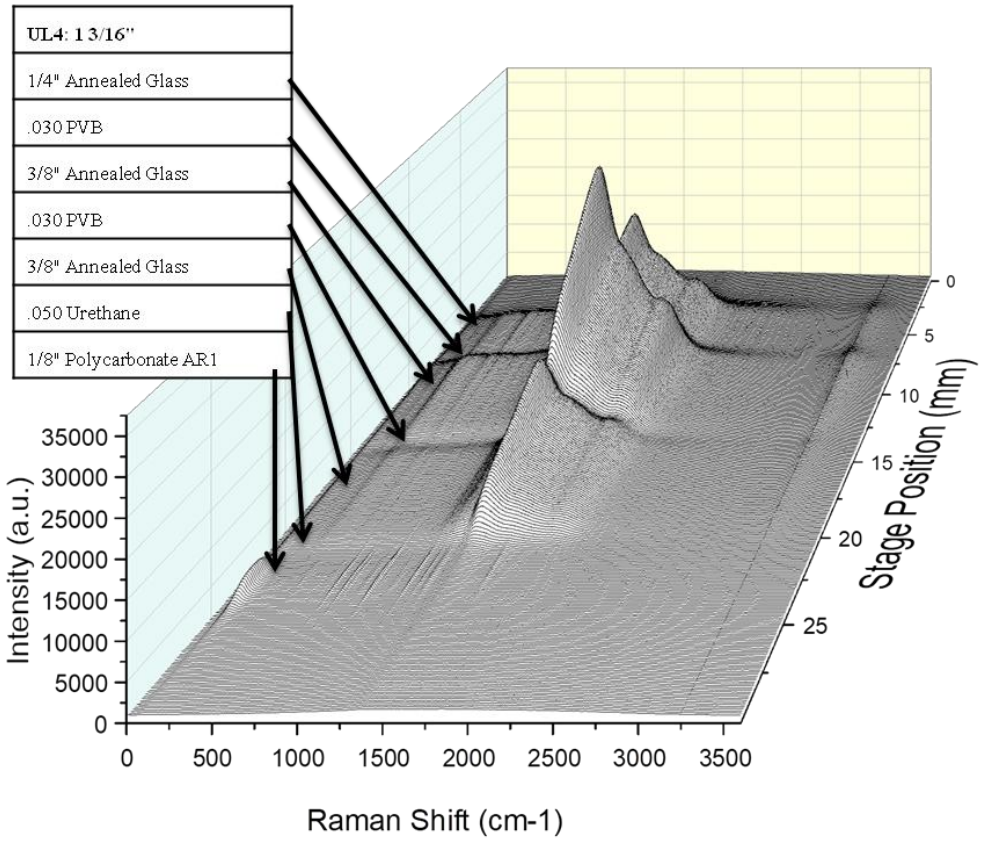

Figure 15. UL 4 Bullet-resistant Glass Raman Depth Profile

UL4 Raman depth profile presented as a 3D waterfall plot. Note the corresponding recipe with the Raman features. The top of the sample or first layer in the sample is the first spectrum recorded and is displayed in the back of the plot beginning at 0 mm. The last layer, the deepest in the sample, is the polycarbonate seen in front by the small but plentiful peaks in the fingerprint region. Each dip between thick layers is a thin layer of adhesive; the adhesives have unique spectral features that are dwarfed by the strong Raman cross-section of the thicker materials such as glass.

The heat map of the Raman intensity displayed from above shows the 4 distinct thick layers. The first layer is clearly visible beginning at stage position 5 and is notably thinner than the other two glass pieces. From this we can conclude that this method is also useful as a thickness measurement. The polycarbonate can most easily be identified by the light portion near 0 wavenumbers and stage position 22-25 mm.

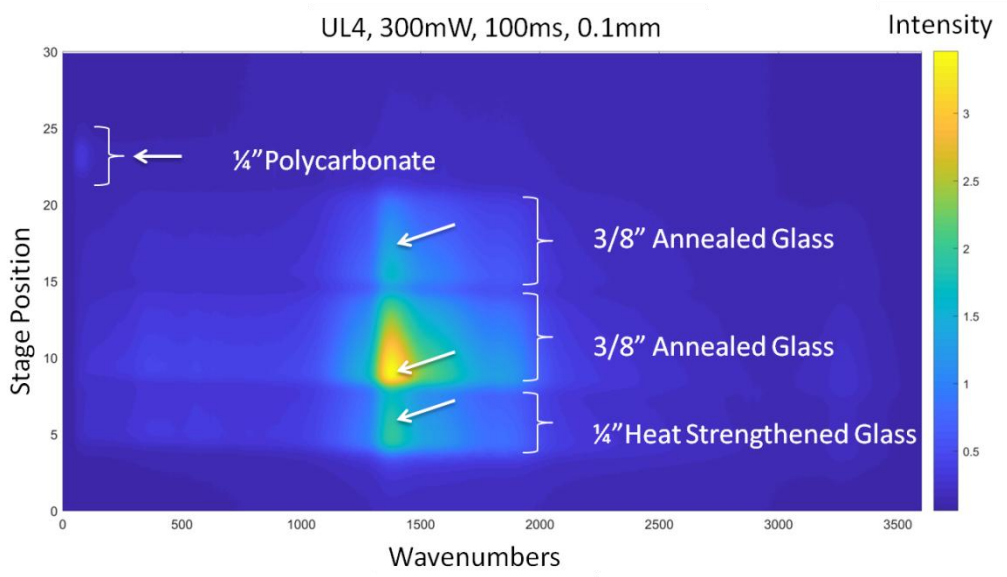

Figure 16. UL4 Raman Depth Profile Heat Map View From Above

In this view the Raman depth profile for each distinct material layer can be easily distinguished by eye.

UL8 is also a commercially available bullet-resistant glass with additional layers for a greater level of protection. In this case a discrepancy between our results and the recipe allowed us to fully demonstrate the usefulness of such a system. The recipe provided by the manufacturer did not match the Raman spectra collected for this sample. The measurements collected reflect a different number of layers and thicknesses of the materials. Comparison of the layers that can be counted in the depth profile with the recipe show that there are five layers of glass, with the thickest located closest to the polycarbonate seen as one layer of peaks in the front of the profile. There is no evidence of 15 layers total in the Raman signal. Polycarbonate can not been seen in the middle of the profile as suggested by the recipe provided by the manufacturer. Based on evidence from the Raman depth profile, it is concluded that the incorrect recipe was provided and

the correct recipe can be created from the Raman data. It was further confirmed by micrometer and visual inspection that the Raman measurements were in fact the correct recipe vs. the recipe provided by the manufacturer, as shown in Figure 17 and Figure 18 and the Raman heat map seen in Figure 19.

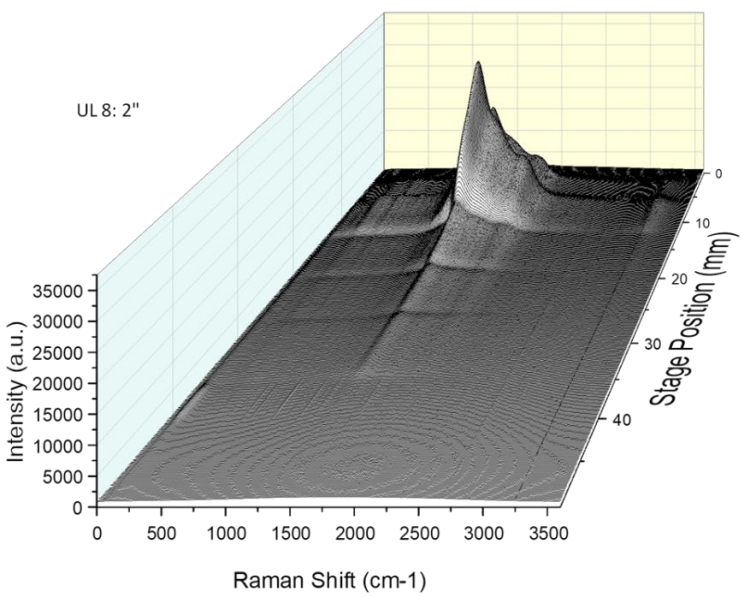

UL 8: 2"-Recipe
1/8" Heat Strengthened Glass
.030 PVB
3/8" Annealed Glass
.030 PVB
3/8" Annealed Glass
.030 PVB
1/4" Annealed Glass
.050 Urethane
1/8" Polycarbonate
.050 Urethane
1/4" Annealed Glass
.050 Urethane
1/4" Polycarbonate AR1
.025 Urethane
1/8" Polycarbonate AR1

UL 8: 2" - Raman
1/4" Heat Strengthened Glass
.030 PVB
3/8" Annealed Glass
.030 PVB
3/8" Annealed Glass
.030 PVB
3/8" Annealed Glass
.030 PVB
12mm Low Iron
.025 Urethane
1/4" Polycarbonate AR1

Figure 17. UL8 Depth Profile and Recipes

UL8 Raman depth profile (left), recipe from manufacturer (middle), Raman data recipe (right).

Figure 18. UL8 Sample Side View

Visually it can be confirmed that UL8 is 5 layers of glass and one layer of polycarbonate annealed with 5 layers of adhesive.

The UL8 sample demonstrates the usefulness of such a device. A technology such as this would be a useful tool for quality assurance. Because it is non-destructive, the product would not be harmed by a confirmation measurement. It is clear that it is capable of these types of measurements.

It could also be used in the field to determine thickness and material of bullet-resistant glass that needs to be destroyed. For example, it would be useful to know the type of material and thickness of material that was obstructing movement. It is reasonable that this tool could be useful in such a situation.

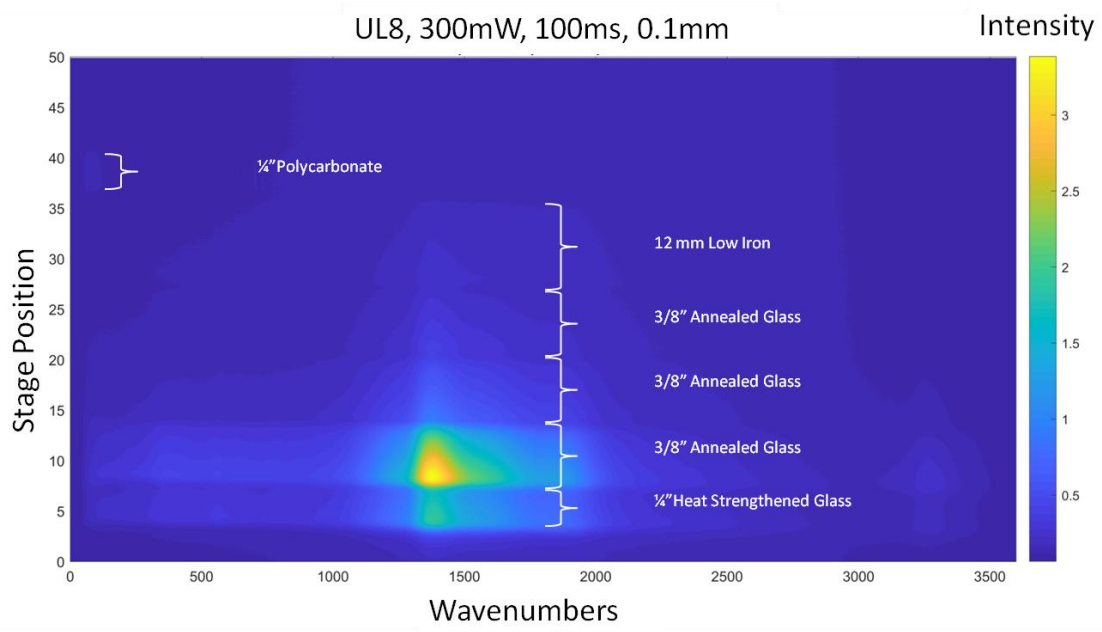

Figure 19. UL8 Raman Depth Profile Heat Map From Above

The Raman depth profile demonstrating 6 layers and 5 adhesive interlayers in UL8.

The remaining four samples are all comprised of the same materials in different orders. It is evident that the Raman system is able to collect sufficient information to identify each layer in order. The data also provides significant information to generate a thickness measurement.

The following images, Figure 20 through Figure 31, display Bullet-resistant Recipe #1 - #4. In addition to a 3D plot of the Raman depth profile, the heat map also displays the unique layers of each stack up. When compared with the provided recipes it becomes clear that this method and the long working distance Raman probe will be a useful tool for characterizing bullet-resistant glass.

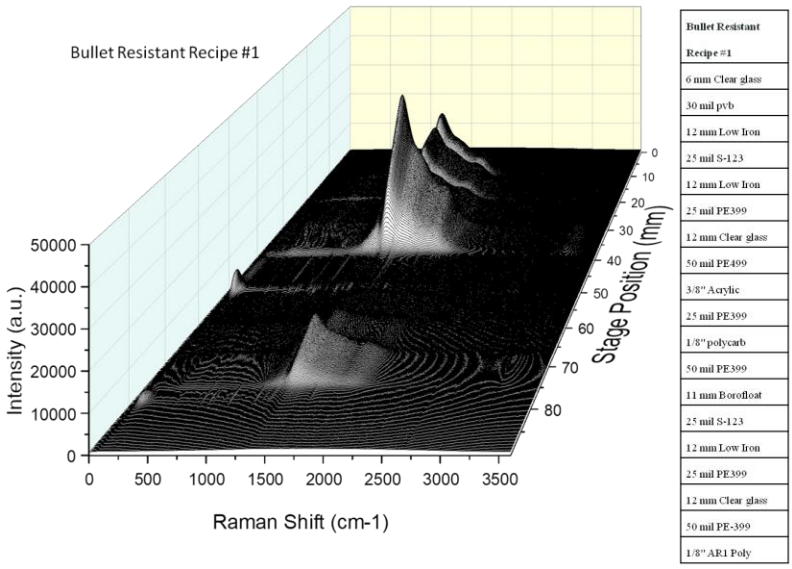

Figure 20. Bullet-resistant Recipe #1 3D Waterfall Plot

A 3D waterfall plot of the Raman depth profile of Bullet-resistant Recipe #1 shows the Raman spectra correlated to each material layer (left) as seen in the recipe (right). Of note, the acrylic signal in the Raman fingerprint region followed by a thinner section of polycarbonate in the middle of the stack up.

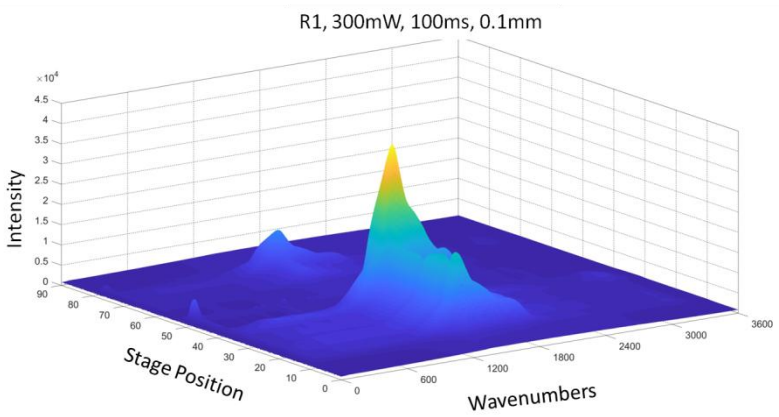

Figure 21. Raman Depth Profile of Bullet-resistant Recipe #1 3D Waterfall Heat Map

A 3D waterfall plot with heat map correlated to Raman signal intensity of the Raman depth profile of Bullet-resistant Recipe #1. Note the strong Raman cross-section of some materials such as 12 mm clear glass.

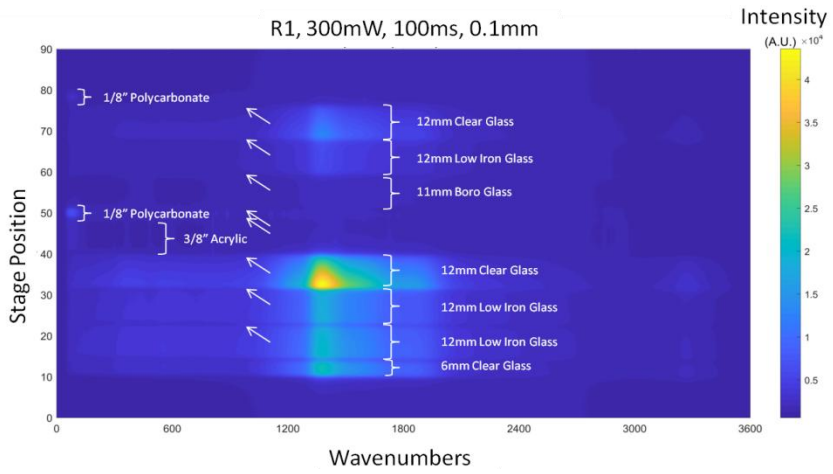

Figure 22. Raman Depth Profile Heat Map of Bullet-resistant Recipe #1 (Top Down)

The Raman depth profile viewed as a heat map from the top looking down, demonstrating 10 layers and 9 adhesive interlayers in Bullet-resistant Recipe #1

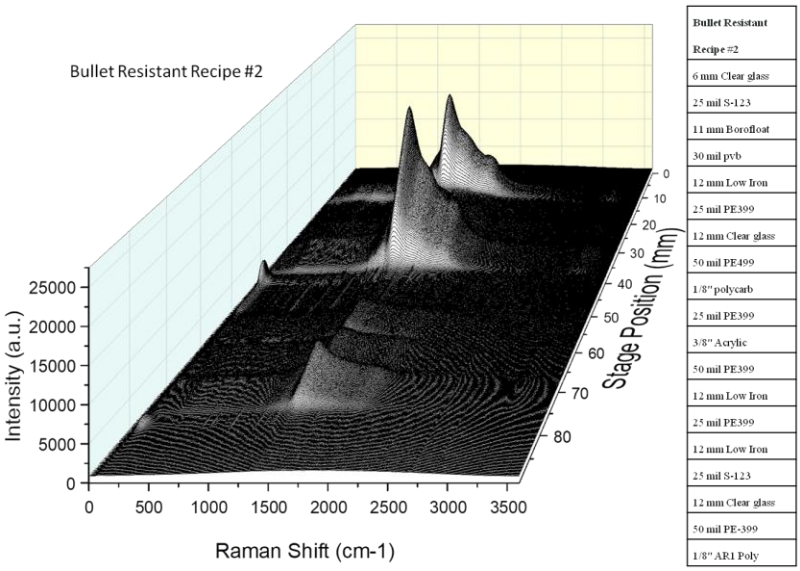

Figure 23. Bullet-resistant Recipe #2 3D Waterfall Plot

A 3D waterfall plot of the Raman depth profile of Bullet-resistant Recipe #2 shows the Raman spectra correlated to each material layer (left) as seen in the recipe (right). Of note, a thin section of polycarbonate followed by a thicker section of acrylic signal in the Raman fingerprint region in the middle of the stack up.

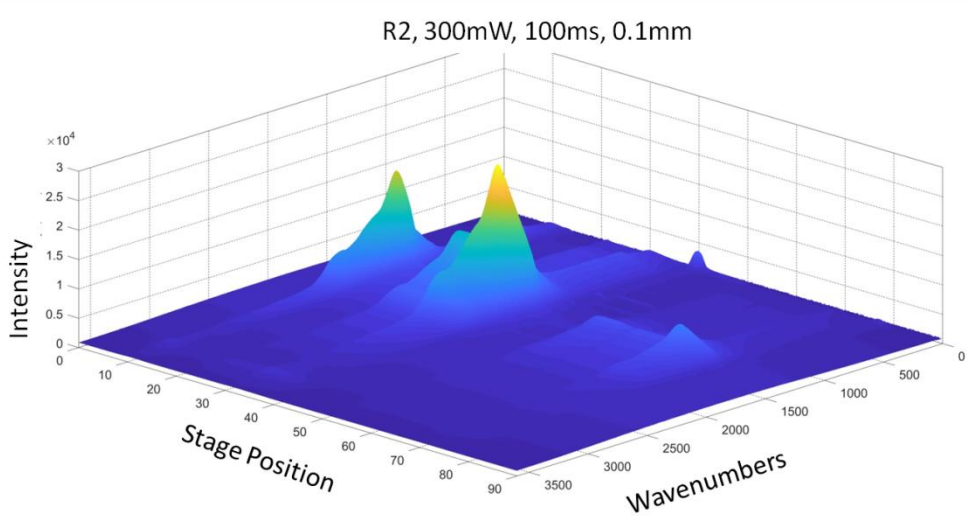

Figure 24. Raman Depth Profile of Bullet-resistant Recipe #2 3D Waterfall Heat Map

A 3D waterfall plot with heat map correlated to Raman signal intensity of the Raman depth profile of Bullet-resistant Recipe #2.

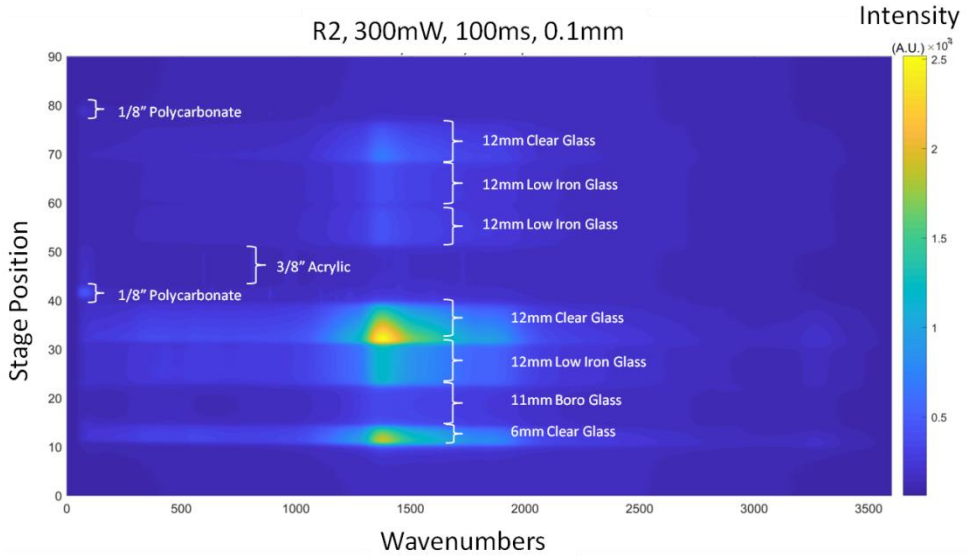

Figure 25. Raman Depth Profile Heat Map of Bullet-resistant Recipe #2 (Top Down)

The Raman depth profile viewed as a heat map from the top looking down, demonstrating 10 layers and 9 adhesive interlayers in Bullet-resistant Recipe #2

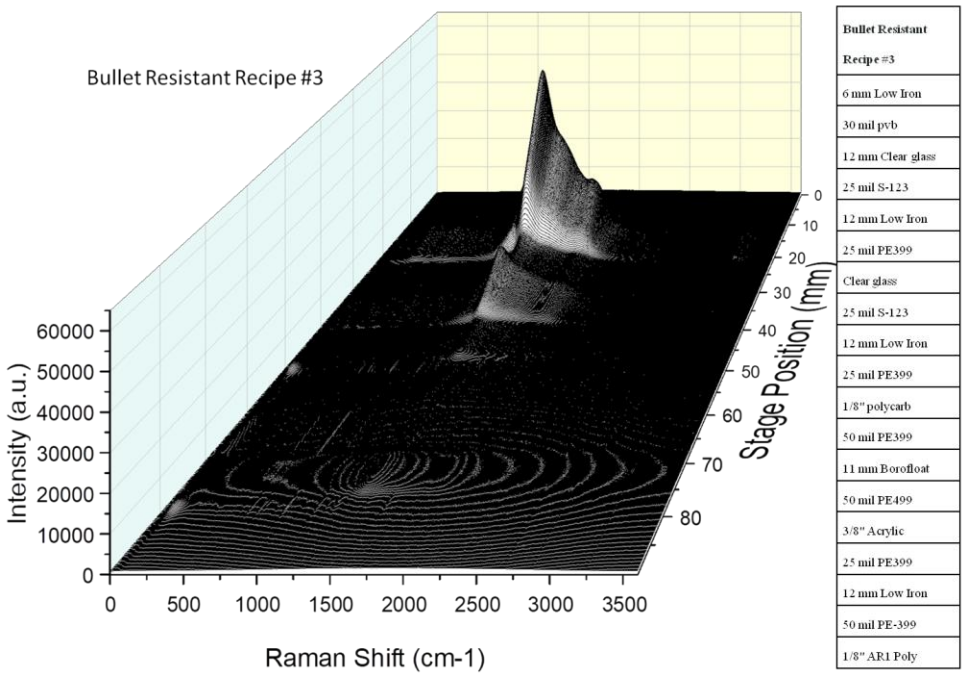

Figure 26. Bullet-resistant Recipe #3 3D Waterfall Plot

A 3D waterfall plot of the Raman depth profile of Bullet-resistant Recipe #3 shows the Raman spectra correlated to each material layer (left) as seen in the recipe (right).

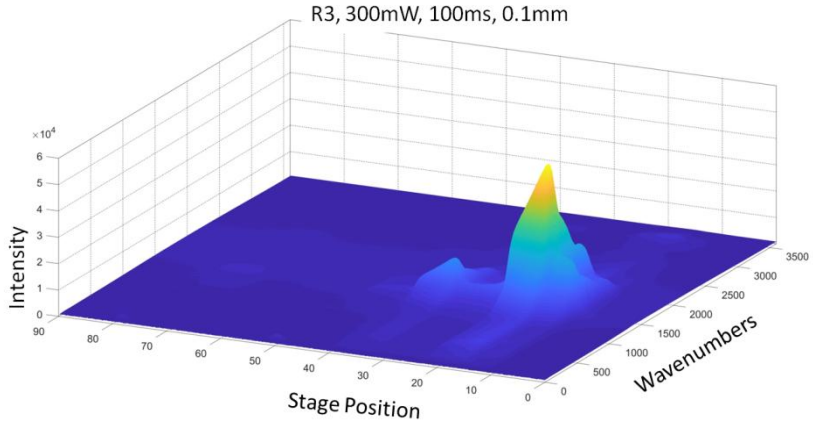

Figure 27. Raman Depth Profile of Bullet-resistant Recipe #3 3D Waterfall Heat Map

A 3D waterfall plot with heat map correlated to Raman signal intensity of the Raman depth profile of Bullet-resistant Recipe #3.

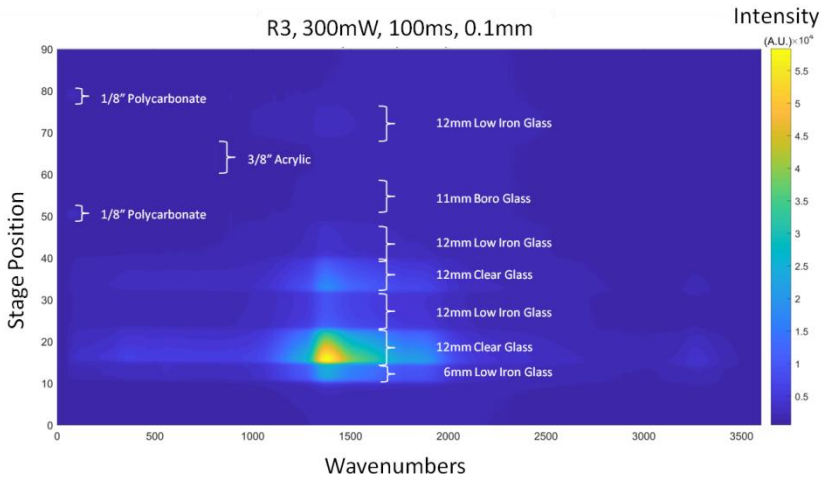

Figure 28. Raman Depth Profile Heat Map of Bullet-resistant Recipe #3 (Top Down)

The Raman depth profile viewed as a heat map from the top looking down, demonstrating 10 layers and 9 adhesive interlayers in Bullet-resistant Recipe #3

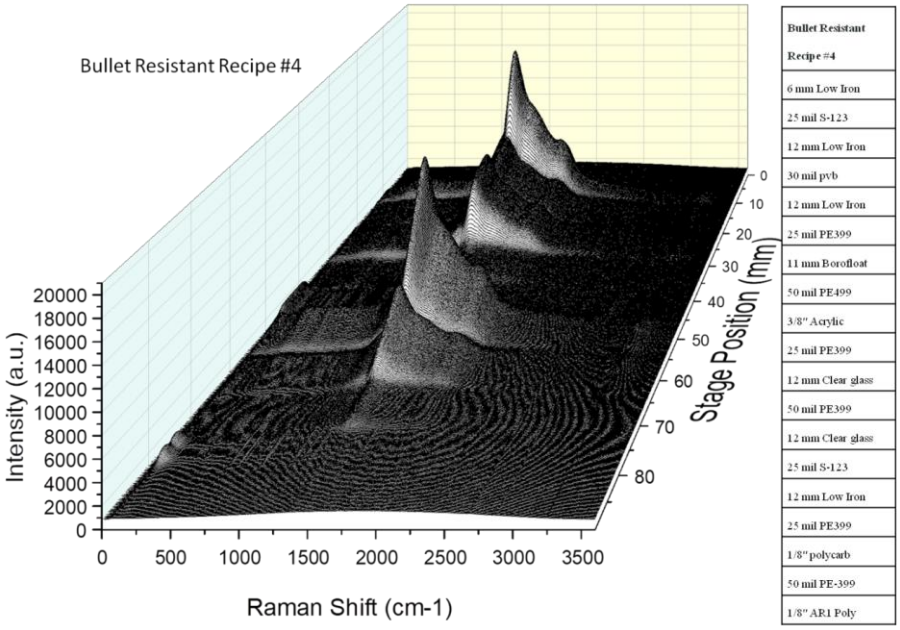

Figure 29. Bullet-resistant Recipe #4 3D Waterfall Plot

A 3D waterfall plot of the Raman depth profile of Bullet-resistant Recipe #4 shows the Raman spectra correlated to each material layer (left) as seen in the recipe (right).

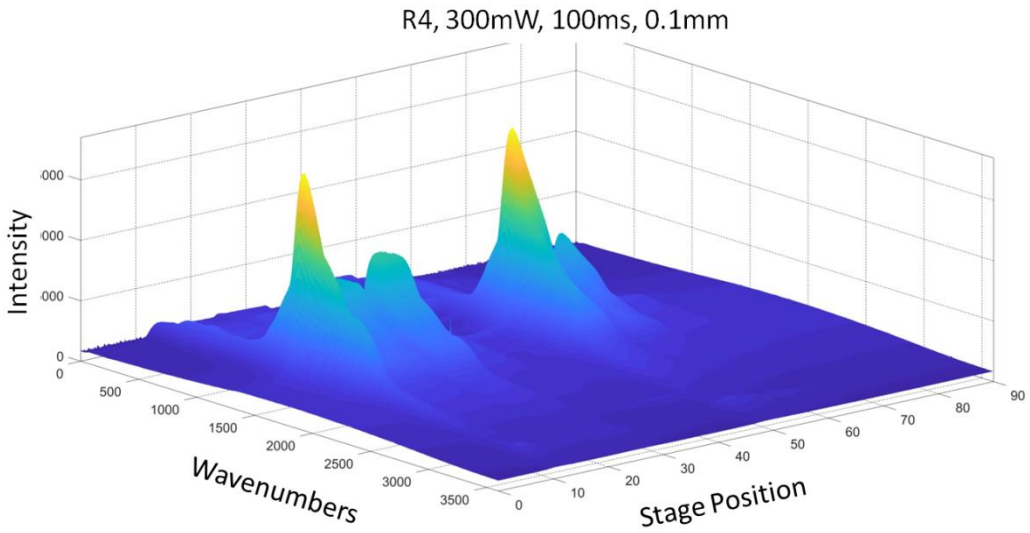

Figure 30. Raman Depth Profile of Bullet-resistant Recipe #4 3D Waterfall Heat Map

A 3D waterfall plot with heat map correlated to Raman signal intensity of the Raman depth profile of Bullet-resistant Recipe #4.

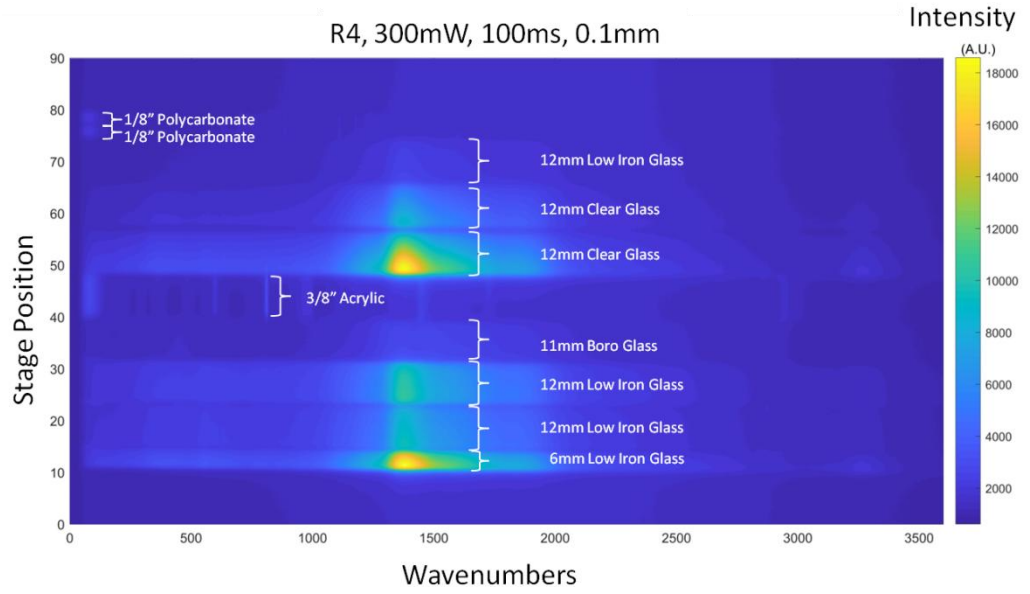

Figure 31. Raman Depth Profile Heat Map of Bullet-resistant Recipe #4 (Top Down)

The Raman depth profile viewed as a heat map from the top looking down, demonstrating 10 layers and 9 adhesive interlayers in Bullet-resistant Recipe #4

The stronger signals dwarf the materials with a smaller Raman cross-section or those deeper in the depth profile, however there is sufficient signal to identify all the layers. For visual clarity, Bullet-resistant Glass Recipe #4 construct provides visually identifiable layers that demonstrate the strength of the Raman spectra. 19 materials are visually identifiable, 10 thick layers and 9 adhesive interlayers in between beginning with a strong soda lime peak all the way up to the two polycarbonate plates in front, each layer separated by a dip in signal of the thin adhesive layer. The adhesive layers also have significant feature to distinguish them, however the overall signal is much smaller than the rest of the Raman depth profile and not visible beyond the dip in signal in these full-size Raman depth profile plots. Figure 31, is a false-color Raman image of adhesive interlayers in a stack up. The bottom of the figure represents the first Raman spectrum collected and the top of the figure represents the last Raman spectrum collected where the polycarbonate plate is located. The data has been plotted from 2800 cm-1 to 3500 cm-1 to focus on the differences in the two types of adhesive in the sample. Note that the adhesive Raman spectral features alternate corresponding to the sequence of adhesives sample. This spectral difference will allow ready identification and differentiation between these adhesives. The layered structure of the bullet-resistant glass construct is obvious in this Raman image.

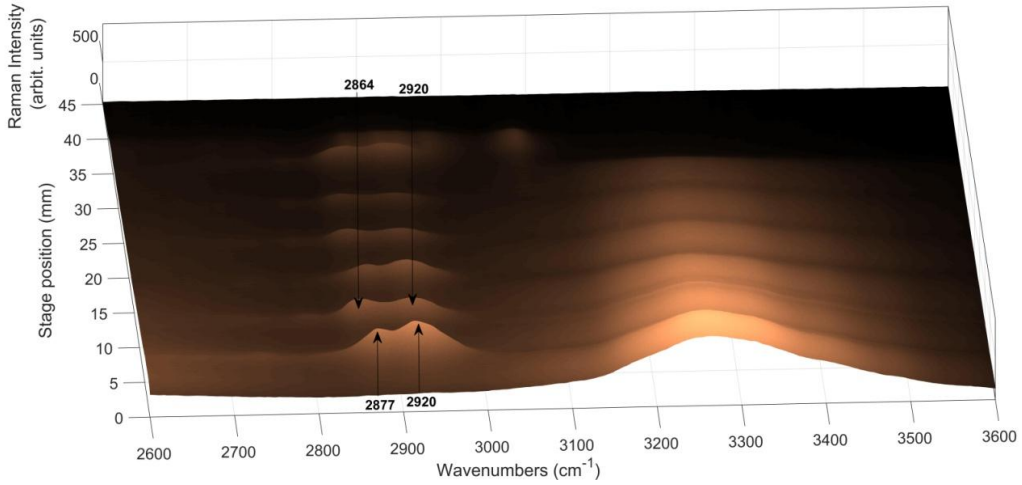

Figure 32. Adhesive Interlayer Features in Raman Depth Profile False Color Plot

In this image, the plot has been cropped and focused on the adhesive layer features. The material is alternating between Urethane PE399 and PVB. Because these two materials have slightly different peaks, they can be distinguished from one another.

In addition to the adhesive layers, in Figure 30 Bullet-resistant Recipe #4, the correlating thicknesses of each material can be seen when comparing the 6 mm section in front with the 12 mm section that follows. The thickness can also be observed in the two 6 mm plates of polycarbonate compared with the other materials.

These Raman depth profiles provide enough information to consider Raman, and in particular a long working distance Raman system, a good tool for characterizing bullet-resistant glass.

Chapter IV

Discussion

The goal of this work was to determine if Raman spectroscopy could be used as a novel technique for characterizing bullet-resistant glass. It has been shown, with the reported results, that a custom designed Raman platform with a long working distance probe would be ideal for these measurements as well as future applications.

Conclusions

It was hypothesized that Raman spectroscopy would be a good technique for measuring thick pieces of bullet-resistant glass. Because of evidence in the literature and preliminary results there was a reasonable assumption of success.

The Raman depth profiling measurement system was able to accurately determine the material in each sample and identify the order in the stack up. Each material had a unique Raman spectrum that could be identified regardless of the location within the bullet-resistant glass construct. Additionally, the data was able to demonstrate varying thicknesses of the materials in the depth profiles.

When analyzing the Raman depth profiles collected with this instrument, each individual material could be identified. It was found that the low iron soda lime glass had a notable different feature than borosilicate glass with a distinct doublet. Both signals had a strong intensity that is appropriate for this kind of analysis. The plastic materials, polycarbonate and acrylic both had strong and unique features in the Raman fingerprint region. This is useful because the features are very different from the broad features in glass. It is additionally useful that the adhesive interlayers have features in the far region

of the spectrum near 2900 cm-1, allowing for clear identification of each material. In addition, it was found the adhesive interlayers have slightly shifted peaks from one another in that region. Based on these findings, as the library of materials expands to include other materials found in bullet proof glass, it can be anticipated that they will be equally well characterized by this technique.

Nearly all the technical risk of this thesis has been diminished with the build and demonstration of the functional platform. The prototype designed and built is extremely effective in measuring bullet-resistant glass. This achievement represents a significant technical effort and supports the thesis while paving the way for future work.

From the results discussed herein, it is apparent that the long working distance Raman probe method would be successful in characterizing any transparent materials from tens of thousandths of an inch to several inches thick. Raman spectroscopy has not been used in this way before and it is reasonable to believe it will be useful in many plausible scenarios in future work.

Further Thickness Measurements

In this report, it has been established that spatially resolved Raman spectra can be correlated to the stage position. However, we have also determined that it is not directly equivalent.

Modeling shows that the laser beam focus spreads out along the optical axis as it penetrates the sample. We can also assume that the returned Raman signal is also significantly affected by the pathway through the sample. Some of these issues can be controlled using other optics such as a pinhole or annulus to exclude particular rays and tighten the focus. In order to determine the solution we must understand the optical

system. This modeling confirms that not all the rays focus at the same place. This can be seen in the following model, Figure 33. Note the outer most ray focuses lower than the central rays.

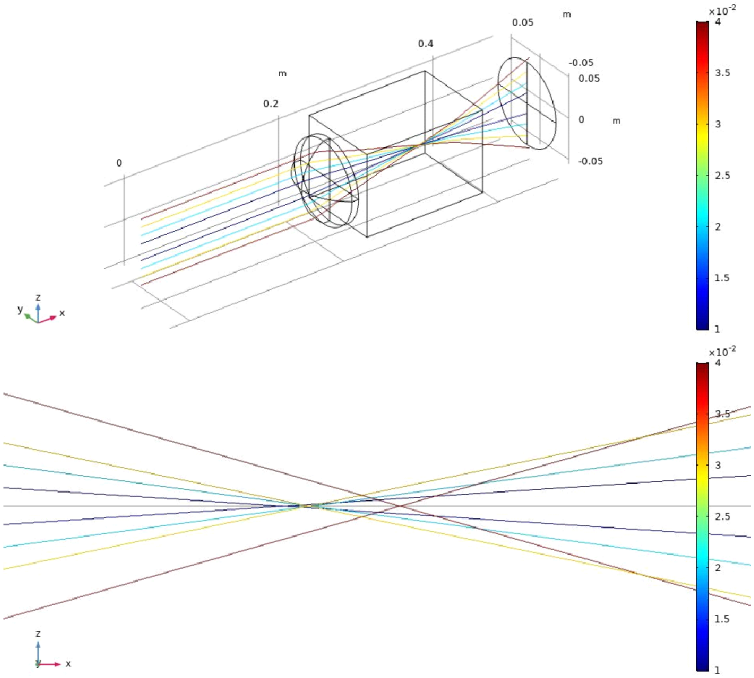

Figure 33. Ray Tracing Through Glass

Focal point in glass (top) Enlarged image of focal point (bottom) Note that in this figure, the outermost ray focuses deeper in the sample as a result of refraction through the glass sample.

The challenge is understanding the effect of the multiple refractive indices on the pathway of the laser beam and thereby the Raman signal. At each interface in a bullet-resistant glass stack up, the rays will be refracted. In order to understand and correct for the outcome, the physics must be explored. In this case Snell's law explains the distortion

of the beam path. Snell's law, Figure 34, is used to describe the relationship between the index of refraction and the angle of incidence of light, in this case the laser beam.

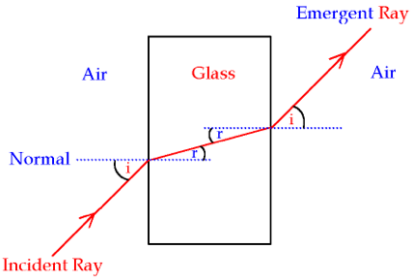

Figure 34. Snell's Law Schematic

Snell's law depicted as a simple ray trace, as the ray moves through multiple refractive indices the path is refracted.

As the laser penetrates through multiple materials, the rays bend and the focal point changes. It is important to note, this is a simplified schematic and in practice there are rays entering from many slightly different angles causing the rays to change their path slightly as they enter different layers. As a result, the focal point of the laser becomes smeared as the rays penetrate deeper into the bullet-resistant sample.

The following images created in SolidWorks demonstrate the concept of Snell's Law and how the ray traces are altered as they penetrate a thick piece of bullet-resistant glass. In air, the focus is sharp and located at its focal length (4"). However, as the focus is moved into the bullet-resistant glass sample it becomes defocused due to refraction occurring at the sample-air interface (Snell's Law). In the figure, a bullet-resistant glass sample is placed 1" below the plano-convex lens L3 in the Raman depth profiling station.

Optical rays emerging from the bottom of the 4” diameter 4” focal length lens L3 are refracted by the bullet-resistant glass sample surface resulting in refocusing of the optical beam. Note the focus location with and without a glass sample in place, seen in Figure 35.

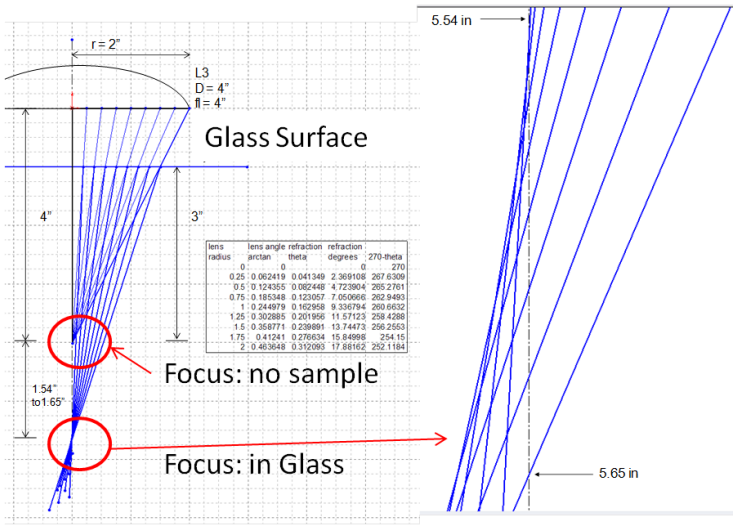

Figure 35. SolidWorks Image of Defocusing Effect

This figure illustrates the defocusing effect of a glass sample (left). An up close view of the defocusing effect is shown on the right. The outer rays are refracted at greater angles at the sample surface to cross the optical axis deeper in the material than the inner rays.

If Snell’s law was not an issue, the distance the probe translates down the stage and the correlated Raman spectra would directly indicate the thickness of the layers. However, by accounting for this refraction the collected data can be accurately translated into actual material thickness measurements. For every millimeter that the probe translates and takes a Raman spectrum, a correction factor will have to be applied to account for the defocusing. Post processing mathematical correction can be applied as has been done in several studies, particular regarding Raman spectra and transparent

materials in “A comparison of different approaches for depth profiling of films and coatings by confocal Raman microscopy” (Miguel, 2012). Future work determining the exact effects of Snell’s law will be necessary.

Future Work

Now that this work has established that it is possible to measure through a four-inch-thick multilayered piece of bullet-resistant glass comprised of a variety of materials there are many avenues of continued research possible. As established, the ability to non-destructively characterize the bullet-resistant glass is a useful tool for quality control when designing and deploying novel and sophisticated constructs. With additional work to establish an accurate account for defocusing, this functional model could be fully automated and commercialized into a deployable unit. In addition, this tool might be useful for forensic analysis. For example, should a bullet-resistant glass fail to withstand a ballistic attack, it would be very useful information to know the composition when determining why it failed and the results of an impact could be characterized. Therefore the system can be envisioned as a forensic lab tool.

Through this study, an additional difficulty with bullet-resistant glass became apparent. Occasionally, bullet-resistant glass fails because of delamination. The adhesive interlayers begin to fog and the window becomes cloudy and less useful for the intended purpose. If the delamination is significant enough, it physically comes apart and compromises the bullet resistance. It is likely that this measurement method would be a great tool for predicting this type of failure as it easily identifies materials such as plasticizers or solvents that may be responsible for the delamination. In addition, the elastic scattering of the laser can be used to quickly identify delamination before it

compromises the bullet-resistant glass. Similarly, it would be a useful analysis tool for measuring the level of wear and tear. It can also be envisioned as quality control for located inclusions in architectural glass. The future work imaginable from this groundwork is plentiful and as the technology advances the possibilities proliferate. The approach of combining modeling, software control and hardware optimization proved to be invaluable in advancing the state of the art of Raman spectroscopy for thick sample depth profiling.

References

Advances in Ceramic Armor III. (2009). In *Advances in Ceramic Armor III*. https://doi.org/10.1002/9780470339695

Bélanger, P. A. (1991). Beam propagation and the ABCD ray matrices. Optics Letters, 16(4), 196. doi:10.1364/ol.16.000196

Bugaev, K. O., Zelenina, A. A., & Volodin, V. A. (2012). Vibrational Spectroscopy of Chemical Species in Silicon and Silicon-Rich Nitride Thin Films. International Journal of Spectroscopy, 2012, 1-5. doi:10.1155/2012/281851

Cakoni, F., Cristo, M. D., & Sun, J. (2012). A multistep reciprocity gap functional method for the inverse problem in a multilayered medium. Complex Variables and Elliptic Equations, 57(2-4), 261-276. doi:10.1080/17476933.2011.625089

Dangwal, V. (2014). Ballistic Simulation Of Bullet Impact on a Windscreen Made of Floatglass and Plexiglass Sheets *International Journal of Aerospace and Mechanical Engineering*. *1*(1), 53–57.

Dispersive Raman Spectrometers. (2005). Raman Spectroscopy for Chemical Analysis, 149-219. doi:10.1002/0471721646.ch8

Esposito, R., Scherillo, G., Pannico, M., Musto, P., De Nicola, S., & Mensitieri, G. (2016). Depth profiles in confocal optical microscopy: a simulation approach based on the second Rayleigh-Sommerfeld diffraction integral. *Optics Express*, *24*(12), 12565. https://doi.org/10.1364/oe.24.012565

Everall, N. J. (2010). Confocal Raman microscopy: Common errors and artefacts. The Analyst,135(10), 2512. doi:10.1039/c0an00371a

Freeguard, G., & Marshall, D. (1980). Bullet-resistant glass: A review of product and process technology. *Composites*, 11(1), 25-32. (n.d.). *No Title*.

Hammoutene, A., Enguehard, F., & Bertrand, L. (1998). Laser-Ultrasonic Optical Characterization of Nonmetals. Review of Progress in Quantitative Nondestructive Evaluation,1419-1426. doi:10.1007/978-1-4615-5339-7_183

Jalham, I. S., & Alsaed, O. (2011). The Effect of Glass Plate Thickness and Type and Thickness of the Bonding Interlayer on the Mechanical Behavior of Laminated Glass. *New Journal of Glass and Ceramics*, *01*(02), 40–48. https://doi.org/10.4236/njgc.2011.12007

Kumar, K., & Monga, I. (2014). An Evaluation of Energy Absorption by Bullet Resistant Glass and its Mechanical Properties. *International Journal for Research in Applied Sciences 2*(Viii), 102–108.

Laser Resonators and Gaussian Beams. (2010). Laser Physics, 269-329. doi:10.1002/9780470409718.ch7

Madden, O., Cobb, K. C., & Spencer, A. M. (2014). Raman spectroscopic characterization of laminated glass and transparent sheet plastics to amplify a history of early aviation "glass." *Journal of Raman Spectroscopy*, *45*(11–12), 1215–1224. https://doi.org/10.1002/jrs.4618

McCarty, K. F. (1987). Raman scattering as a technique of measuring film thickness: interference effects in thin growing films. *Applied Optics*, *26*(20), 4482. https://doi.org/10.1364/ao.26.004482

Miguel, M. D. L. P., & Pablo Tomba, J. (2012). A comparison of different approaches for depth profiling of films and coatings by confocal Raman microscopy. *Progress in Organic Coatings*, *74*(1), 43–49. https://doi.org/10.1016/j.porgcoat.2011.09.016

Nicolais, L., Zang, M. Y., & Chen, S. H. (2011). Laminated Glass. *Wiley Encyclopedia of Composites*, (October 2017). https://doi.org/10.1002/9781118097298.weoc121

Pershin, S. M., Lednev, V. N., Yulmetov, R. N., Klinkov, V. K., & Bunkin, A. F. (2015). Transparent material thickness measurements by Raman scattering. *Applied Optics*, *54*(19), 5943. https://doi.org/10.1364/ao.54.005943

Vitro Architectural Glass PPG. (2014). Heat Treated Glass for Architectural Glazing. *Glass Technical Document TD-138*, (January), 1–5.

Strassburger, E., Hunzinger, M., Mccauley, J., & Patel, P. (2010). Experimental Methods for Characterization and Evaluation of Transparent Armor Materials. Ceramic Engineering and Science Proceedings Advances in Ceramics Armor VI,183-198. doi:10.1002/9780470944004.ch16

Subhash, G. (2013). Transparent Armor Materials. Experimental Mechanics,53(1), 1-2. doi:10.1007/s11340-012-9689-y

Weller, B., Wünsch, J., & Härth, K. (2005). Experimental study on different interlayer materials for laminated glass. *Glass Processing Days*, (January 2005).